EUROPEAN ORGANIZATION FOR NUCLEAR RESEARCH (CERN)

CERN-EP-2026-091
2026/08/14

CMS-HIG-25-018

Search for Higgs boson pair production in the $b\bar{b}WW$ decay channel with two leptons in the final state using proton-proton collision data at $\sqrt{s} = 13.6\,\text{TeV}$

The CMS Collaboration*

arXiv:2604.02127v2 [hep-ex] 13 Aug 2026

Abstract

A search for Higgs boson pair production is presented, targeting final states where one Higgs boson decays to a bottom quark-antiquark pair and the other Higgs boson decays to two W bosons, both of which decay leptonically, to an electron or a muon, and a neutrino. For the first time, the search is conducted with proton-proton collision data from the LHC at $\sqrt{s} = 13.6\,\text{TeV}$, recorded with the CMS detector in 2022 and 2023 and corresponding to an integrated luminosity of $62\,\text{fb}^{-1}$. The results are consistent with the standard model predictions. An upper limit of 12.0 times the standard model prediction at 95% confidence level is set on the Higgs boson pair production cross section, with an expected limit of 18.5. The results are also used to constrain the strength of the trilinear self-coupling of the Higgs boson, as well as of the quartic coupling between two Higgs bosons and two vector bosons.

Published in the Journal of High Energy Physics as doi:10.1007/JHEP08(2026)019.

© 2026 CERN for the benefit of the CMS Collaboration. CC-BY-4.0 license

*See Appendix A for the list of collaboration members

1 Introduction

The measured properties of the Higgs boson (H) discovered [1–3] by the ATLAS and CMS Collaborations at the CERN LHC are consistent with the expectations of the standard model (SM) Brout–Englert–Higgs (BEH) mechanism [4–11] within the current experimental precision [12, 13]. One aspect of the BEH mechanism that is largely unknown experimentally is the exact shape of the Higgs potential, which, in the SM, is related to the trilinear self-coupling of the Higgs boson and can be directly probed using Higgs boson pair (HH) production [14]. In the SM, the dominant HH production mode at the LHC is gluon-gluon fusion (ggF), followed by vector boson fusion (VBF) production, with cross sections of $34.1^{+2.2}_{-7.9}$ fb [15–17] and 1.87 ± 0.05 fb [18, 19], respectively, at the centre-of-mass energy ($\sqrt{s}$) of 13.6 TeV for a Higgs boson mass of 125 GeV. The VBF production mode is furthermore sensitive to the quartic coupling between two Higgs bosons and two vector bosons [20]. Representative Feynman diagrams of HH production in the ggF and VBF modes are shown in Fig. 1.

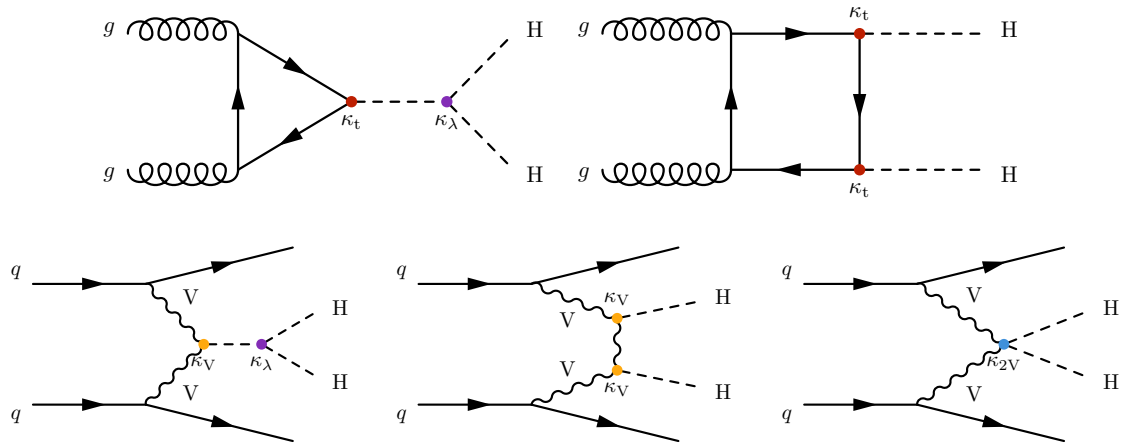


Figure 1: Leading-order Feynman diagrams of HH production in the ggF production mode assuming top quarks in the fermion loop (top row) and in the VBF production mode (bottom row) in the SM.

The HH production process has not yet been observed. Previous searches for HH production have been performed by the ATLAS and CMS Collaborations with LHC Run 2 data at 13 TeV in various final states and their combinations [21–23]. Recently, the ATLAS Collaboration also published a search for HH production in the final state with a bottom quark-antiquark pair ($b\bar{b}$) and two photons, combining both LHC Run 2 and Run 3 data at 13 TeV and 13.6 TeV, respectively [24].

This article presents a search for non-resonant HH production, targeting final states where one Higgs boson decays to $b\bar{b}$ and the other Higgs boson decays to two W bosons, both of which decay leptonically to an electron or a muon, and a neutrino. Previous searches in the $b\bar{b}WW$ channel with the Run 2 data set were performed by the CMS Collaboration in final states with one or two leptons, setting an observed (expected) upper limit on the inclusive HH production cross section of 14 (18) times the SM prediction at 95% confidence level (CL) [25], and by the ATLAS Collaboration in the two-lepton final state with an upper limit of 9.7 (16.2) times the SM prediction at 95% CL [26].

In this search, events are selected with exactly two oppositely charged leptons ($\mu^+\mu^-$, e^+e^-, $e^\pm\mu^\mp$). The selected events are categorised based on the output of a multiclassification neural network (NN) into several regions targeting HH signal events from ggF or VBF production, or

background events from different processes. The categorisation is further refined based on the b-tagged jet multiplicity and the presence of a jet from a Lorentz-boosted $H \to b\bar{b}$ candidate. The events in the signal-enriched regions are then classified by dedicated binary NNs designed to separate ggF or VBF signal events from background events. The output distributions of the binary NNs, together with the event yield in the background-enriched regions, enter the final fit as sensitive observables. An upper limit is set on the inclusive HH production cross section, and the result is used to constrain the strength of the trilinear Higgs boson self-coupling as well as the quartic coupling between two Higgs bosons and two vector bosons. Throughout this article, the values of the Higgs boson couplings are expressed in terms of coupling modifiers κ, denoting the coupling strength relative to the SM prediction [27]. The modifier of the trilinear coupling is denoted by κ_λ, and that of the quartic coupling by κ_{2V}.

Several refinements have been implemented relative to the previous search [25]. A new classification strategy, utilising a staged multiclassification-plus-binary NN approach, resulted in an improvement in sensitivity of approximately 50%, evaluated as the exclusion limit expected with a dataset of the same size as used in Ref. [25]. Furthermore, an improved trigger strategy for e^+e^- ($e^\pm\mu^\mp$) events led to an increase of the signal yield in this channel by 5% (1%) inclusively and up to 17% (3%) in the most signal-like bins of the final discriminant distribution. Finally, an improved b tagging algorithm was used, and the analysis benefits from the higher centre-of-mass energy of Run 3, resulting in a 5% increase in the ratio of signal events to the square root of the number of background events.

This article is structured as follows. The CMS detector as well as the object and event reconstruction are described in Section 2, followed by a description of the data and the simulated event samples in Section 3. The event selection and the analysis strategy are detailed in Section 4, and systematic uncertainties are discussed in Section 5. The statistical analysis and the results obtained are presented in Section 6. Finally, a summary is provided in Section 7. Tabulated results are provided in the HEPData record for this analysis [28].

2 The CMS detector and event reconstruction

The CMS apparatus [29, 30] is a multipurpose, nearly hermetic detector, designed to trigger on [31–33] and identify muons, electrons, photons, and (charged and neutral) hadrons [34–36]. Its central feature is a superconducting solenoid of 6 m internal diameter, providing a magnetic field of 3.8 T. Within the solenoid volume are a silicon pixel and strip tracker, a lead tungstate crystal electromagnetic calorimeter (ECAL), and a brass and scintillator hadron calorimeter, each composed of a barrel and two endcap sections. Forward calorimeters extend the pseudorapidity coverage provided by the barrel and endcap detectors. Muons are reconstructed using gas-ionisation detectors interleaved with the layers of the steel flux-return yoke outside the solenoid. More detailed descriptions of the CMS detector, together with a definition of the coordinate system used and the relevant kinematic variables, can be found in Refs. [29, 30]. A global "particle-flow" (PF) algorithm [37] aims to reconstruct all individual particles in an event, with an optimised combination of information from the various elements of the CMS detector. The reconstructed particles are used to build jets and missing transverse momentum (p_T^{miss}) [38, 39].

Events of interest are selected using a two-tiered trigger system. The first level, composed of custom hardware processors, uses information from the calorimeters and muon detectors to select events at a rate of around 100 kHz within a fixed latency of 4 μs [31]. The second level, known as the high-level trigger, consists of a farm of processors running a version of the full event reconstruction software optimised for fast processing, and reduces the event rate to a few

kHz before data storage [32, 33].

The reconstruction of muons relies on a combination of measurements in the tracker and in the muon detectors [35]. The muons are identified based on the quality of the combined track fit and on the number of hits in the different tracking detectors, with an efficiency of about 90%, including the isolation requirements described below. The transverse momentum (p_T) resolution in the barrel is better than 1% (7%) for muons with p_T up to 100 GeV (1 TeV) [35]. Muons are required to lie within the acceptance of the muon system, covering pseudorapidity (η) values of $|\eta| < 2.4$, and to have $p_T > 25$ and 15 GeV for the p_T-leading and subleading muons, respectively.

Electrons are reconstructed by combining the momentum measurement in the tracker with the energy measurement of the corresponding cluster in the ECAL and with the energy sum of all bremsstrahlung photons, obtained from the ECAL, spatially compatible with originating from the electron track [34, 40]. The electrons are identified using criteria on the cluster shape in the ECAL, the track quality, and the compatibility between the tracker and ECAL measurements, corresponding to an identification efficiency of approximately 80%, including the isolation requirements described below. The momentum resolution for electrons with p_T of about 45 GeV ranges from 1.6 to 5% [34, 40]. Electrons are required to have $|\eta| < 2.5$ as well as $p_T > 25$ and 15 GeV for the p_T-leading and subleading electrons, respectively. Electrons reconstructed in the transition region $1.44 < |\eta| < 1.56$ between the barrel and the endcap calorimeters are discarded.

Isolation requirements are imposed on the muons and electrons with the aim of suppressing leptons originating from decays of heavy hadrons inside jets. The isolation is based on the scalar p_T sum of all PF objects in a cone of radius 0.3 in the η-ϕ plane around the track direction of the lepton, where ϕ denotes the azimuthal angle, and it is corrected by removing contributions arising from additional proton-proton (pp) interactions in the same or an adjacent bunch crossing (pileup) [41].

Hadronic jets are clustered from the PF objects using the anti-k_T algorithm [42, 43] with a distance parameter of 0.4 (jets) and of 0.8 (large-radius jets). No matching is performed between jets and large-radius jets, but they are treated as independent objects; thus, a large-radius jet will typically also appear as one or several corresponding jets in the event. The pileup-per-particle identification algorithm (PUPPI) [41, 44] is used to mitigate the effect of pileup at the reconstructed-particle level. Jet energy corrections are applied to bring the measured response of jets to that of particle level jets on average [38]. The jet energy resolution amounts typically to 15–20% at 30 GeV, 10% at 100 GeV, and 5% at 1 TeV [38]. Jets (large-radius jets) overlapping within a cone of radius 0.4 (0.8) in the η-ϕ plane with a muon or an electron passing the criteria described above are discarded. For the analysis, jets and large-radius jets with $|\eta| < 2.4$ as well as with $p_T > 25$ GeV and $p_T > 200$ GeV, respectively, are selected.

In addition, jets with $|\eta| > 2.4$ (forward jets) are used in the identification of HH production via the VBF process, which is characterised by the presence of jets with large $|\eta|$ values. Jets that are less (more) forward with $2.4 < |\eta| < 3$ ($|\eta| > 3$) and $p_T > 50$ GeV ($p_T > 30$ GeV) are selected. Out of all the jets and the forward jets that are not used for the $H \to b\bar{b}$ reconstruction, all possible pairs are selected, and the pair with the largest pseudorapidity gap $\Delta\eta$ is referred to as the VBF jet pair. An event is considered as VBF tagged if the VBF jet pair has $\Delta\eta > 3$ and an invariant dijet mass larger than 500 GeV.

Jets arising from the hadronisation of b quarks (b jets) are identified using the ParticleNet tagging algorithm [45–47]. Jets are considered as b tagged if they fulfil a requirement on the

PARTICLENET discriminant that corresponds to a b tagging efficiency of approximately 80% and a 1% (14%) misidentification probability for light-flavour quark and gluon (charm quark) induced jets. The PARTICLENET algorithm is further used to identify Higgs bosons with large p_T decaying to $b\bar{b}$ [45, 48]. Large-radius jets are considered as boosted $H \to b\bar{b}$ candidate jets if they fulfil a requirement on the PARTICLENET discriminant that corresponds to an efficiency of approximately 26% (22%) of identifying $H \to b\bar{b}$ jets for ggF (VBF) production, with a background misidentification rate of 2%. The b jet [49, 50] and the $H \to b\bar{b}$ jet [48] (mis)identification probabilities are corrected to match the efficiencies measured in data.

3 Data and simulated event samples

Data from pp collisions at $\sqrt{s} = 13.6\,\text{TeV}$ collected in 2022 and 2023, corresponding to an integrated luminosity of $62\,\text{fb}^{-1}$, are analysed. The data are reconstructed separately in four different data-taking periods with different detector conditions—$8\,\text{fb}^{-1}$ and $27\,\text{fb}^{-1}$ of the data collected in 2022 as well as $18\,\text{fb}^{-1}$ and $10\,\text{fb}^{-1}$ of the data collected in 2023—and appropriate per-period calibrations are applied before the data are combined for the analysis. The simulated events described in the following are generated accordingly in four different samples for each physical process, reflecting the different data-taking conditions.

Signal and background events are modelled using the Monte Carlo (MC) event generators POWHEG v2.0 [51–54] or MADGRAPH5_aMC@NLO v2.9.13 [55], interfaced with a detailed detector simulation based on GEANT4 [56]. The proton structure is described by the parton distribution function (PDF) set NNPDF3.1 [57] at next-to-next-to-leading order (NNLO) precision in quantum chromodynamics (QCD) perturbation theory. Parton showering (PS) and hadronisation are simulated with PYTHIA v8.306 [58], where the parameters for the underlying event description correspond to the CP5 tune [59]. For comparison with the observed distributions, the events in the simulated samples are normalised to the same integrated luminosity as the data sample, according to their predicted cross sections. Pileup effects are modelled by adding simulated minimum bias events to all simulated events with a frequency distribution adjusted to match that observed in the data.

The HH signal process in the ggF production channel is simulated at next-to-leading order (NLO) precision in QCD with POWHEG [60, 61]. Samples with different values of κ_λ are generated, allowing the kinematic distributions for different κ_λ values to be modelled using a weighted sum of the samples [14]. Signal events in the VBF production channel are generated with MADGRAPH5_aMC@NLO at leading-order (LO) precision. Samples with different values of κ_λ and κ_{2V} are produced, allowing the kinematic distributions to be modelled for each (κ_λ, κ_{2V}) configuration, following the same principle as for the ggF samples. The resulting inclusive HH cross section for each value of the coupling modifiers is normalised to a calculation at NNLO precision in QCD [15–17]. All relevant HH decay modes are considered, with relevant contributions arising from $b\bar{b}WW$, $b\bar{b}\tau\tau$, and $b\bar{b}ZZ$.

The final state targeted by this search is dominated by background processes from top quark-antiquark ($t\bar{t}$) and single top quark (single-t/$\bar{t}$) production, as well as $Z/\gamma^* + \text{jets}$, referred to as Drell–Yan (DY) production. The overall normalisation of the $t\bar{t}$ and DY processes are measured in situ in the final fit to data described in Section 6.

The $t\bar{t}$ background process is simulated at NLO precision in QCD using POWHEG [62]. The top quark p_T spectrum in the POWHEG simulation has been found to be harder than the one observed in data. This is attributed to missing higher-order calculations [63, 64], and therefore the simulated events are reweighted to match the prediction at NNLO precision in QCD

and NLO precision in electroweak corrections [65]. The corrections at 13 TeV are taken from Ref. [65], and an additional small correction is applied to extrapolate them to 13.6 TeV, following Ref. [66]. The inclusive cross section is normalised to a calculation at NNLO precision in QCD including resummation of next-to-next-to-leading logarithmic soft-gluon terms [67–73].

The single-$t/\bar{t}$ background is dominated by tW production, with small additional contributions from single top quark production in the t and s channels. The processes are simulated at NLO precision in QCD, for tW production and in the t channel with POWHEG [74, 75], and in the s channel with MADGRAPH5_aMC@NLO. The inclusive cross section of the tW process is normalised to calculations at approximate NNLO precision [76], and the t and s channel processes to predictions at NLO precision [77, 78].

The DY background process is simulated with up to two partons at the matrix element (ME) level at NLO precision in QCD with MADGRAPH5_aMC@NLO, where the merging of the jets from the ME calculation and the PS is done using the FXFX [79] prescription. Dedicated corrections, described later in Section 4.4, are derived from data to improve the modelling of relevant observables, such as the jet multiplicity spectrum in DY events. The DY events are separated into two mutually exclusive processes, based on the flavour of the jets at the particle level, where these jets fulfil the acceptance requirements of $p_{\mathrm{T}} > 20\,\mathrm{GeV}$ and of $|\eta| < 2.4$. Events with at least one particle-level jet that contains one or more b- or c-flavoured hadrons are classified as DY + heavy-flavour jets (DY + HF) events, and all other events are classified as DY + light-flavour and gluon jets (DY + LF) events.

Minor background contributions arise from the resonant production of single Higgs bosons (H production). The H production processes in the ggF and VBF channels, associated production with a vector boson (VH), ZH production in ggF, and $\mathrm{t\bar{t}}$ associated production are simulated at NLO precision using POWHEG [80–84]. Associated $\mathrm{t\bar{t}VH}$ production is simulated at NLO precision using MADGRAPH5_aMC@NLO, and single-$t/\bar{t}$ associated H production in the tHq and tHW channels is simulated at LO precision using MADGRAPH5_aMC@NLO. Their cross sections are normalised to the latest available calculations, taken from Ref. [16].

Further minor background contributions stem from W + jets production, the production of two (VV) or three (VVV) Z or W bosons, $\mathrm{t\bar{t}}$ production in association with one ($\mathrm{t\bar{t}V}$) or two ($\mathrm{t\bar{t}VV}$) Z or W bosons, and from the production of four top quarks ($\mathrm{t\bar{t}t\bar{t}}$). They are simulated using POWHEG [85] (VV, VVV) and MADGRAPH5_aMC@NLO (W + jets, $\mathrm{t\bar{t}V}$, $\mathrm{t\bar{t}VV}$, $\mathrm{t\bar{t}t\bar{t}}$).

4 Event selection and analysis strategy

Events are selected with exactly two oppositely charged leptons ($\mu^+\mu^-$, $\mathrm{e^+e^-}$, $\mathrm{e^\pm}\mu^\mp$). The selected events are categorised into several signal regions (SRs), targeting ggF and VBF production, or into background control regions (CRs), based on the output of a multiclassification NN as well as the b-tagged jets multiplicity and the presence of a boosted $\mathrm{H} \to \mathrm{b\bar{b}}$ candidate jet. The events in the SRs are classified by additional NNs designed to separate ggF or VBF signal events from background events. The distributions of the output values of the binary NNs in the SRs, together with the event yield in the CRs, enter the final fit as sensitive observables.

Contributions from SM background processes are modelled using the simulated events described in Section 3. Dedicated corrections are derived for the DY events to improve the modelling of the data, and the normalisations of the dominant $\mathrm{t\bar{t}}$ and DY background processes are determined in the final fit to data.

The event selection, the analysis strategy, the details of the NN architecture and training, as

well as the background modelling are detailed in the following, and the analysis strategy is illustrated in Fig. 2.

4.1 Event selection

The data are selected using a combination of triggers. The triggers require the presence of either one or two muon candidates for the $\mu^+\mu^-$ events, one or two electron candidates for the e^+e^- events, as well as one muon or one electron candidate, or one muon and one electron candidate, for the $e^\pm\mu^\mp$ events. The minimal thresholds on the trigger objects are $p_T > 8\,\text{GeV}$ for the muons and $p_T > 12\,\text{GeV}$ for the electrons. The trigger selection for e^+e^- and $e^\pm\mu^\mp$ events features an inefficiency at lepton p_T above 100 GeV owing to an electron isolation criteria employed in the electron triggers. This is compensated by using additional triggers with looser electron isolation criteria that require the presence of two electrons with $p_T > 33\,\text{GeV}$ or of one electron with $p_T > 50\,\text{GeV}$ and one jet with $p_T > 165\,\text{GeV}$. The latter criteria are new compared to the previous search [25]. As a result, the total selection efficiency with respect to the offline reconstruction achieved for signal events after the event selection described below is 98% in the $\mu^+\mu^-$ channel, 95% in the e^+e^- channel, and 96% in the $e^\pm\mu^\mp$ channel. The single-lepton triggers and the two new triggers contribute up to 12% to the signal selection efficiency, depending on the channel.

A further offline selection, referred to as the baseline selection, requires events to have exactly two muons or two electrons or one muon and one electron of opposite charge, and at least one b-tagged jet. Events are rejected if further muons or electrons are present with $p_T > 5$ or 7 GeV, respectively. Events must be accepted by a trigger based on online leptons with a flavour consistent with that of the two leptons selected offline; for example, $\mu^+\mu^-$ events are required to pass a dimuon or single-muon trigger. The invariant mass of the selected lepton pair, $m_{\ell\ell}$, is required to be larger than 20 GeV to suppress events from heavy-flavour resonance decays and low-mass DY processes.

The selected events are then separated into an analysis region with $20 < m_{\ell\ell} < 70\,\text{GeV}$ and $p_T^{\text{miss}} > 40\,\text{GeV}$ as well as into validation regions with $m_{\ell\ell} > 110\,\text{GeV}$, enriched in $t\bar{t}$ events, and with $70 < m_{\ell\ell} < 110\,\text{GeV}$ for e^+e^- and $\mu^+\mu^-$ events, enriched in DY events. The analysis region events are used in the final analysis to extract the signal, and the validation region events are used to verify the $t\bar{t}$ and DY background modelling and derive corrections for the DY background. The total selection efficiency for $HH \to b\bar{b}WW$ signal events in final states with two leptons (e^+e^-, $\mu^+\mu^-$, or $e^\pm\mu^\mp$) in the analysis region is 12%.

The event selection criteria are summarised in Table 1.

4.2 Analysis strategy

The events in the analysis region are categorised in several steps, as illustrated in Fig. 2. First, the events are categorised by a multiclassification NN (NN_{cat}) designed to separate between different signal and background processes. The values obtained in the output nodes of the NN_{cat} are normalised to unity using a "soft-max" function, and, as a result, the output values can be interpreted as probabilities describing the likelihood of the event being of a certain process. Events are assigned to the category corresponding to the most probable process according to this NN multiclassification. The events are separated into one of two SRs targeting ggF HH production (SR_{ggF}) or VBF HH production (SR_{VBF}), or into one of four background CRs targeting the main background processes: $t\bar{t}$, single-$t/\bar{t}$, DY, and H production.

Events in SR_{ggF} and SR_{VBF} are further sorted into one of three categories, according to their

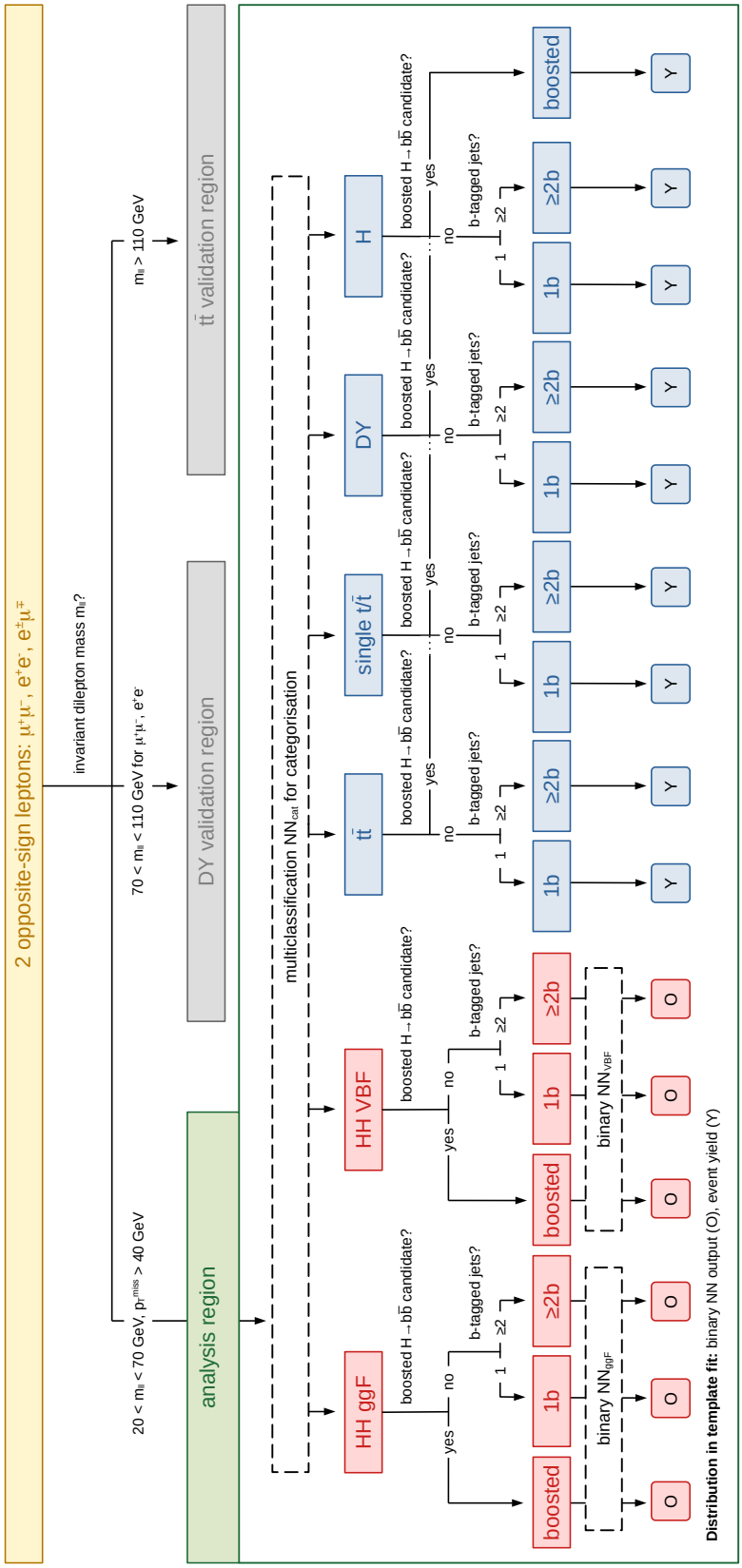


Figure 2: Illustration of the event categorisation: SRs are depicted in red, background CRs in blue. Details of the NNs are described in the text. The binary NN output distributions (O) and the event yields (Y) in the CRs enter the final fit as sensitive observables.

Table 1: Event selection criteria in the analysis region (AR) and the DY and $t\bar{t}$ validation regions (VR).

	Baseline selection		
Number of leptons	2		
p_T of leading lepton	>25 GeV		
p_T of subleading lepton	>15 GeV		
$\|\eta\|$ of electrons	<2.5		
$\|\eta\|$ of muons	<2.4		
Number of jets	≥ 1		
Number of b-tagged jets	≥ 1		
p_T of jets	>25 GeV		
$\|\eta\|$ of jets	<2.4		
	AR	DY VR	$t\bar{t}$ VR
Sign and flavour of leptons	$\mu^+\mu^-$, e^+e^-, $e^\pm\mu^\mp$	$\mu^+\mu^-$, e^+e^-	$\mu^+\mu^-$, e^+e^-, $e^\pm\mu^\mp$
$m_{\ell\ell}$	20–70 GeV	70–110 GeV	>110 GeV
p_T^{miss}	>40 GeV		

jet content: events containing a boosted $H \to b\bar{b}$ candidate jet are sorted into the "boosted" categories $SR_{ggF}^{boosted}$ and $SR_{VBF}^{boosted}$; events containing exactly one b-tagged jet are sorted into the "1b" categories SR_{ggF}^{1b} and SR_{VBF}^{1b}; and the remaining events containing two or more b-tagged jets are sorted into the "$\geq$2b" categories $SR_{ggF}^{\geq 2b}$ and $SR_{VBF}^{\geq 2b}$. Events in the CRs are sorted into a dedicated boosted category if a boosted $H \to b\bar{b}$ candidate jet is present. There is one single such category for all CR events owing to the low number of events. The remaining CR events are sorted into the 1b ($\geq$2b) categories if they contain exactly 1 ($\geq$2) b-tagged jets. This results in 15 categories in total: three categories (boosted, 1b, $\geq$2b) in each of the two SRs (SR_{ggF}, SR_{VBF}), two categories (1b, $\geq$2b) in each of the four CRs, and a boosted CR.

The events in the three SR_{ggF} categories are further classified by a dedicated binary NN (NN_{ggF}), which is optimised to separate ggF production HH events from the inclusive background. The output values of the NN_{ggF} are used as discriminating observables in the SR_{ggF} categories in the final fit. Likewise, the events in the three SR_{VBF} categories are classified by another binary NN (NN_{VBF}) optimised to separate VBF production HH events from the background, and the output values of the NN_{VBF} are used as final discriminating observables. The binning in the SR_{ggF} (SR_{VBF}) categories is chosen such that the NN_{ggF} (NN_{VBF}) output distributions are uniform for ggF (VBF) signal events, and such that the uncertainty due to the limited number of simulated events is sufficiently small. In the background CRs, the yield in each category enters the final fit. The resulting discriminant distribution is shown in Fig. 5 in Section 6.

The analysis strategy has been optimised using simulated events to achieve the best sensitivity. For example, the inclusion of the dedicated boosted categories improves the expected limit on the SM HH production cross section by 4% and reduces the confidence interval on κ_{2V} by 26%.

4.3 Neural network architecture and training

The hyperparameters [86] of the multiclassification NN_{cat} and the binary NN_{ggF} and NN_{VBF} are listed in Table 2. They have been optimised based on the achieved expected limit to SM HH production, evaluated on simulated events.

Table 2: Hyperparameters of the neural networks. Where they differ for the multiclassification NN_{cat} and the binary NN_{ggF} and NN_{VBF}, they are listed as "$NN_{cat}/NN_{ggF}/NN_{VBF}$", otherwise they are the same for all networks.

Hidden layers	3
Nodes per hidden layer	512
Activation function	ReLU
Output activation function	Softmax
Loss function	Categorical cross-entropy
Preprocessing	Batch normalisation
Dropout rate	20%
Training epochs	100
Batch size	4032/10648/15972
Steps per epoch	52/23/15
Initial learning rate	5×10^{-4}
Learning rate decay	0.8
Learning rate decay patience	3 epochs

The NNs are trained using simulated signal and background events from all four analysed data-taking periods together, thereby reducing statistical fluctuations in the trained NN parameter values. The events are weighted to reflect the different integrated luminosities. The sensitivity of the analysis does not degrade compared to the case of training NNs separately for each data-taking period or when using information about the period of data taking as an input feature to the NNs.

Simulated signal events with different values of κ_λ and κ_{2V} are used for the training. For ggF production, four different samples are used with values of κ_λ of 0, 1, 2.45, and 5, and for VBF production, six different samples are used with values of κ_λ and κ_{2V} between -3.39 and 1 and between 0.959 and 3.57, respectively. The values have been chosen to represent regions in parameter space with distinct kinematic properties. For example, at $\kappa_\lambda = 0$, there is no contribution from diagrams involving the trilinear Higgs boson self-coupling (Fig. 1 top left) and HH production proceeds via the diagram involving only couplings between the top quark and the Higgs boson (Fig. 1 top right), while at $\kappa_\lambda = 2.45$, the destructive interference between the two types of diagrams is maximal, such that the HH production cross section is minimal. For the training of the binary NNs, only HH signal events of the target production process are considered. For example, for the training of the NN_{ggF}, only the ggF production HH events are used as signal, while the VBF production HH events do not enter the training.

Events from the different simulated samples are effectively weighted during training to prevent the NN classification from being biased by the relative frequencies of the underlying processes. For signal events, the weighting is chosen such that the different simulated κ_λ and κ_{2V} points have the same effective number of events, obtained as the sum of all weights, in each batch

used for training. For background events in the $\mathrm{NN_{cat}}$ training, the weighting is chosen such that each background process has the same effective number of events as the total effective number of signal events. In the binary NN trainings, the background events are weighted relative to each other by the cross section of the processes. However, a larger relative weight is assigned to the events of some of the minor background processes in order to avoid large statistical fluctuations from few events in the analysis bins with largest signal purity. Finally, the total effective number of background events is normalised to the total effective number of signal events. This scheme has been chosen in order to find a compromise between sensitivity to the SM HH signal, to κ_λ, and to $\kappa_{2\mathrm{V}}$, evaluated by the expected limits, as well as to minimise the size of MC statistical uncertainties.

A five-fold cross-validation technique is used for the training and evaluation of the NNs. In each fold, the 80% of events used for training are further split into three independent subsamples used for the actual training (75%), for the optimisation of the hyperparameters (10%), and for validating the performance of the NNs (15%). The training is terminated after 100 epochs.

The input variables of the NNs are listed in Table 3. The same variables are used in the multiclassification and in the binary NNs, with the exception of the VBF tag information, which only enters the $\mathrm{NN_{VBF}}$. No dedicated input variables based on the properties of the boosted $\mathrm{H} \to \mathrm{b\bar{b}}$ candidate jets are considered. The input variables have been chosen out of a larger set of possible observables as the ones that are most important for the performance of the NNs, based on several ranking procedures including a "data Shapley" metric [87] and the expected limit on the SM HH production cross section. The exact importance ranking of each variable varies for the different NNs. As an example, four input variables with generally high importance based on the data Shapley metric are shown in Fig. 3: the invariant mass and the p_T of the H candidate decaying to $\mathrm{b\bar{b}}$, reconstructed as the invariant mass and p_T, respectively, of the two jets with the highest b tagging score; the invariant mass of the HH system, reconstructed as the invariant mass of the two jets with the highest b tagging score, the two leptons, and $p_\mathrm{T}^\mathrm{miss}$; and the p_T of the jet with the highest b tagging score.

4.4 Background modelling

All background processes are modelled using the simulated event samples described in Section 3, with the corrections and calibrations discussed in the previous sections. The overall normalisation of the $\mathrm{t\bar{t}}$ and the DY background processes are free parameters in the final fit to data. Two separate $\mathrm{t\bar{t}}$ normalisation parameters are assigned, one for the 1b and $\geq$2b categories, and one for the boosted categories, in order to account for potential modelling differences in the two very different p_T regimes. For the DY background, two separate normalisation parameters are assigned, one to the DY + HF and one to the DY + LF process, to account for flavour-dependent effects in the hadronic part of the events.

The background modelling of the dominant $\mathrm{t\bar{t}}$ and DY background processes is verified in the $\mathrm{t\bar{t}}$ validation region with $m_{\ell\ell} > 110\,\mathrm{GeV}$ and in the DY validation region with $70 < m_{\ell\ell} < 110\,\mathrm{GeV}$ for $\mathrm{e^+e^-}$ and $\mu^+\mu^-$ events, respectively. While the relevant observables are sufficiently well modelled for $\mathrm{t\bar{t}}$ events, a mismodelling is observed for DY events, in particular in the distribution of the jet multiplicity, N_jets, as well as in the p_T spectrum of the dilepton system, $p_\mathrm{T}^{\ell\ell}$. Therefore, a dedicated correction of the DY events is derived as a function of $p_\mathrm{T}^{\ell\ell}$ and N_jets, using the data in the DY validation region.

The DY correction is determined from $\mu^+\mu^-$ events in the DY validation region, which has a purity of 94%, using the following procedure. The $p_\mathrm{T}^{\mu\mu}$ distribution observed in data, after subtraction of the expected non-DY contribution predicted by simulation, is divided by the $p_\mathrm{T}^{\mu\mu}$

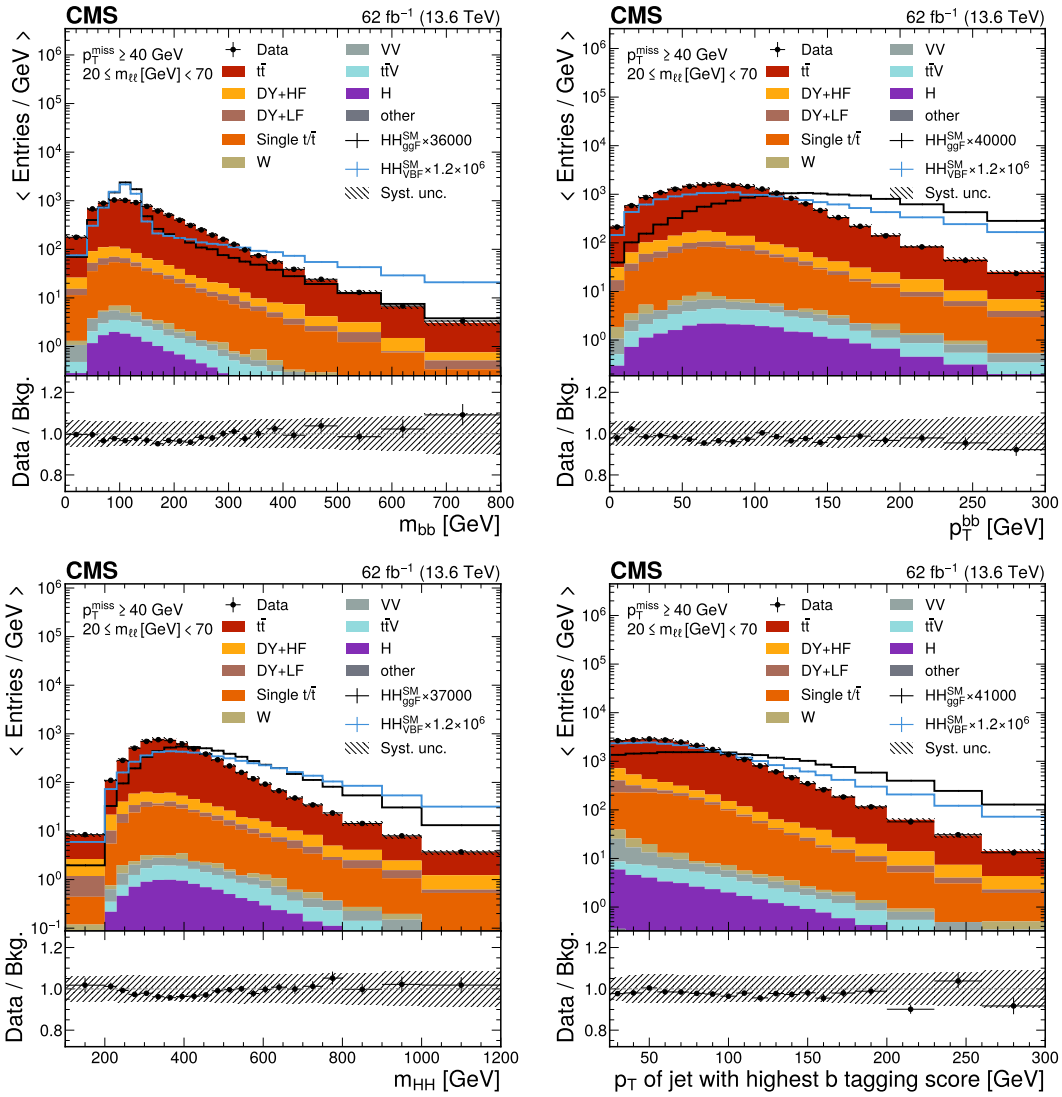


Figure 3: Invariant mass (upper left) and p_T (upper right) of the H candidate decaying to $b\bar{b}$, reconstructed as the invariant mass and p_T, respectively, of the two jets with the highest b tagging score; invariant mass of the HH system (lower left), reconstructed as the invariant mass of the two jets with the highest b tagging score, the two leptons, and p_T^{miss}; and p_T of the jet with the highest b tagging score (lower right), for events in the analysis region observed in data (markers) and predicted by the background model (stacked histograms) prior to the fit to data. The HH signal distributions in the ggF and VBF production channels as predicted in the SM, scaled to the total background yield for better visibility, are overlaid (solid lines). The uncertainty band represents the total systematic uncertainty.

Table 3: Observables used as input variables to the NNs.

Invariant mass of $\mathrm{b\bar{b}}$ system†; proxy for the mass of the $\mathrm{H} \to \mathrm{b\bar{b}}$ candidate
Invariant mass of $\ell\ell$ system ($m_{\ell\ell}$)
Invariant mass of the leptons and $p_{\mathrm{T}}^{\mathrm{miss}}$; proxy for the mass of the $\mathrm{H} \to \mathrm{WW}$ candidate
Invariant mass of the b jets†, leptons, and $p_{\mathrm{T}}^{\mathrm{miss}}$; proxy for the mass of the HH system
Number of jets
Scalar sum of jet p_{T} (H_{T})
p_{T} of jet with highest b tagging score
p_{T} of jet with second-highest b tagging score
p_{T} of leading jet that is not considered as part of the $\mathrm{b\bar{b}}$ system†
p_{T} of the $\mathrm{b\bar{b}}$ system†
Sum of b tagging scores of all jets
p_{T} of leading lepton
p_{T} of subleading lepton
p_{T} of the $\ell\ell$ system
η of leading jet that is not considered as part of the $\mathrm{b\bar{b}}$ system†
Maximum ΔR between jets
ΔR between jets of $\mathrm{b\bar{b}}$ system†
ΔR between leptons
ΔR between $\mathrm{b\bar{b}}$ system† and $\ell\ell$ system
Minimum ΔR between lepton and b-tagged jet
$p_{\mathrm{T}}^{\mathrm{miss}}$
Binary tag of lepton flavour combinations: same flavour or mixed flavour
Binary VBF tag based on the presence of a VBF jet pair ‡

† two jets with highest b tagging scores; in events with only one jet, the observable is assigned a non-physical default value of -10

‡ only used in $\mathrm{NN_{VBF}}$

distribution predicted by the DY simulation, and the resulting ratio is parameterised using an empirical function $f_{\mathrm{DY}}^{\mathrm{corr}}(p_{\mathrm{T}}^{\ell\ell})$. Then, $f_{\mathrm{DY}}^{\mathrm{corr}}$ is applied as an event weight to the simulated DY events in the analysis region as a function of the particle-level $p_{\mathrm{T}}^{\ell\ell}$, correcting the simulated $p_{\mathrm{T}}^{\ell\ell}$ spectrum to match the data. Applying the correction as a function of the particle-level $p_{\mathrm{T}}^{\ell\ell}$ avoids dilution due to the electron momentum resolution, while for the muons the effect of the p_{T} resolution is negligible. The correction $f_{\mathrm{DY}}^{\mathrm{corr}}$ is derived separately for events with $N_{\mathrm{jets}} = 1$ and $N_{\mathrm{jets}} \geq 2$, and for the latter, an additional normalisation factor is applied per N_{jets} bin to

account for residual mismodelling of the jet multiplicity. The correction derived in the DY validation region is applicable also in the analysis region, since the relative fraction of DY + HF and DY + LF events is the same in both regions. The effect of the corrections is demonstrated in Fig. 4, which shows the $p_{\mathrm{T}}^{\mathrm{ee}}$ distribution in $\mathrm{e^+e^-}$ events in the DY validation region before and after application of the corrections. The robustness of the correction procedure has been carefully verified, for example by testing different correction functions and by deriving dedicated corrections per data-taking period, leading to results consistent with those of the nominal method.

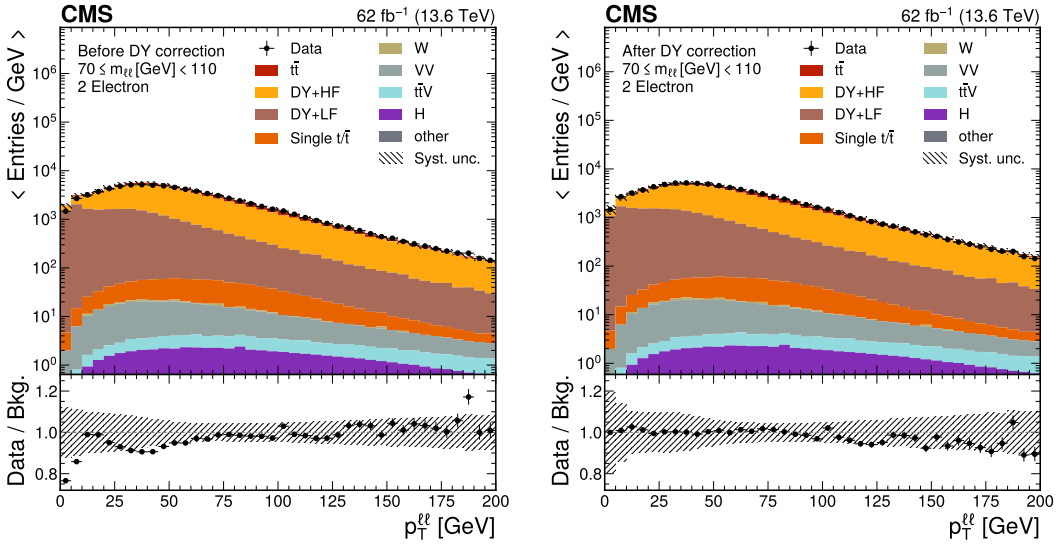


Figure 4: The p_{T} of the dilepton system in the $\mathrm{e^+e^-}$ channel in the DY validation region before (left) and after (right) application of the DY corrections. The uncertainty band shows the total systematic uncertainty.

5 Systematic uncertainties

The sensitivity of the analysis is primarily limited by statistical uncertainties. However, several sources of systematic uncertainties also affect the result and have been considered as described in the following. The systematic uncertainties alter either the rate or both the rate and the shape of the discriminant distributions for the signal or background processes. Their impact on the measured signal and background yields is discussed in Section 6.

Theoretical uncertainties are treated as fully correlated among the different data-taking periods, while experimental uncertainties are in most cases treated as uncorrelated between the periods. The latter assumption is motivated by the fact that the experimental uncertainties are mainly of statistical origin related to the limited size of the data and simulation samples used in auxiliary measurements, which are independent across the data-taking periods, and that the detector conditions changed between the data-taking periods.

Uncertainties in the inclusive cross sections used to predict the rate of the signal and background processes arise primarily from variations of the renormalisation and factorisation scales and the PDFs, as well as the treatment of the top quark mass in case of the signal in the ggF production channel, and are propagated to the yield estimates. The cross section uncertainties are each separated into a component ($\sigma(\mu_{\mathrm{R}}/\mu_{\mathrm{F}})$) due to the renormalisation (μ_{R}) and factorisation (μ_{F}) scales, or scales and top quark mass ($\sigma(\mu_{\mathrm{R}}/\mu_{\mathrm{F}} + m_{\mathrm{t}})$) for signal, and a component due to

the PDF ($\sigma(\text{PDF} + \alpha_S)$). The uncertainties are correlated where appropriate among processes; for example, for processes with the same dominant initial state, such as $t\bar{t}Z$ and $t\bar{t}t\bar{t}$, the PDF uncertainties are treated as correlated. Since the normalisation of the $t\bar{t}$ and DY background processes are measured in situ, they are not affected by the uncertainties of the inclusive cross section predictions. For the signal, the uncertainties in the inclusive cross section prediction generally affect the result since the measured rate is normalised to the SM expectation.

Uncertainties in the simulation of the signal and background events are evaluated as follows. Uncertainties arising from missing higher-order terms at the ME level are evaluated from variations of the μ_R and μ_F scales by factors of 2 and 0.5 with respect to the nominal values. All possible permutations of independent scale variations are performed, excluding the two extreme variations where one scale is varied by a factor of 2 and the other by a factor of 0.5, and the envelope of the six obtained variations in the fitted distributions is assigned as the uncertainty ($\mu_{R/F}$ scale) [88]. The uncertainty originating from the PDF set is determined from the PDF variations provided with the NNPDF3.1 set [57], following the procedure described in Ref. [89], correlating processes for which the same flavour scheme and order in α_S are used in the PDF set. The uncertainty in the PYTHIA PS is determined by varying the parameters controlling the amount of initial- and final-state radiation independently by factors of 2 and 0.5 with respect to their nominal value [58]. The initial-state radiation uncertainties are treated as correlated among the processes, while the final-state radiation uncertainties are treated as uncorrelated between the processes. Uncertainties in the corrections applied to the p_T spectrum of the top quarks in the $t\bar{t}$ simulation [63] are also considered; they amount up to 7% of the expected yield depending on the p_T of the top quarks.

The theory modelling uncertainties described in the previous paragraph arising in the simulation of the events can affect the overall normalisation, the detector acceptance, and the shapes of the fitted distributions. For the $t\bar{t}$ and DY background processes, whose normalisations are determined in the fit, the impact of these variations on the inclusive normalisation (i.e., before any event selection) is removed, leaving only acceptance and shape effects. Likewise, for the other processes, the variation in the normalisation is removed in order to avoid double counting with the uncertainty in the inclusive cross section prediction used to predict the rates of the processes.

Effects of the uncertainty in the distribution of the number of pileup interactions are evaluated by varying the total inelastic cross section used to predict the number of pileup interactions in the simulated events by $\pm 4.6\%$ from its nominal value [41]. The uncertainties in the integrated luminosity used to normalise the predicted signal and background yields are 1.4% for 2022 [90] and 1.3% for 2023 [91].

The trigger efficiency is measured in an unbiased sample of events, mostly $t\bar{t}$ leptonic decays, that contain two leptons and fulfil the offline event selection criteria but were collected with triggers based on p_T^{miss}, which feature a negligible correlation with the triggers used in this analysis. Corrections are derived to match the efficiency in simulation to that observed in data, with uncertainties of up to 5%, dominated by statistical fluctuations in the data samples used in the measurement.

Residual differences between the lepton reconstruction, identification, and isolation efficiencies in data and simulation are corrected based on efficiency measurements using a "tag-and-probe" method in data samples of $Z \to \ell\ell$ events [34, 35]. The uncertainties are smaller than 1 and 2% for the muon and electron correction factors, respectively.

The uncertainties in the jet energy scale and resolution are propagated by varying the correc-

tions applied to all jets in the signal and background simulations within their uncertainty [38]. The uncertainties in the corrections of the b jet (mis)identification probabilities in simulated events [49, 50], which can arise from the contamination of background processes in the data samples used for their derivation, are considered separately for light-flavour quark and gluon jets, b jets, and c jets, and vary between 5 and 30%, depending on the jet p_{T}. Uncertainties in the correction of the boosted $\mathrm{H} \to \mathrm{b\bar{b}}$ candidate jet tagging efficiency amount to approximately 5%, and are considered separately for the boosted ggF and VBF SRs and the boosted CR.

The uncertainty in the DY spectrum correction is evaluated as half of the difference between the nominal and the corrected distributions, and applied symmetrically to the corrected distributions. It has been verified that the size of the uncertainty does not bias the result of the analysis.

The impact of statistical fluctuations in the signal and background prediction due to the limited number of simulated events (MC stat unc.) is accounted for using the Barlow–Beeston "lite" approach [92].

6 Results

A simultaneous binned profile likelihood fit of the signal and background templates to the observed discriminant distributions in all categories is performed, using the CMS statistical analysis tool COMBINE [93]. Each template includes the events of all data-taking periods. The rates of the $\mathrm{t\bar{t}}$ and DY background processes described in Section 4.4 are free parameters in the fit, and the systematic uncertainties described in Section 5 are taken into account via nuisance parameters in the likelihood function. Log-normal distributions are used to model the effects of nuisance parameters on the overall rate. Shape uncertainties are implemented through an interpolation between alternative templates [92, 93], obtained by propagating the effect of the uncertainties to the input variables of the NNs and then evaluating the NNs using the varied inputs. Uncertainties that are decorrelated between different data-taking periods are implemented by varying only the fractional contributions corresponding to the data-taking periods in each template. The observed yields in each bin of the final discriminant distributions in all channels and categories are shown in Fig. 5.

The goodness-of-fit is quantified using a p-value that takes into account the postfit uncertainty model [93] and amounts to $p = 0.19$, indicating good description of the data by the fit model. The best fit value of the $\mathrm{t\bar{t}}$ background normalisation parameter is $0.95^{+0.03}_{-0.02}$ ($0.82^{+0.08}_{-0.07}$ in the boosted categories), consistent with a dedicated $\mathrm{t\bar{t}}$ cross section measurement in a similar phase space region [94].

No significant excess of events over the background-only hypothesis is observed. Upper limits on the cross section of non-resonant Higgs boson pair production are set at 95% CL under the background-only hypothesis, using the $\mathrm{CL_s}$ criterion [95, 96] and assuming asymptotic distributions [97] of the profile likelihood ratio test statistics defined in Ref. [93]. The observed upper limit on the inclusive HH production cross section normalised to the value expected in the SM (HH signal strength modifier) is 12.0, with a median expected limit of 18.5. The observed limit is lower than the expected limit, which can be attributed to a downward fluctuation in the observed event counts relative to the background prediction in several bins, most notably in the most sensitive $\mathrm{SR_{ggF}}$ bin (bin 16 in Fig. 5).

The limit on the HH production cross section is also shown as a function of κ_λ and as a function of $\kappa_{2\mathrm{V}}$ in Fig. 6, where in each case all other couplings are assumed to conform to the SM predic-

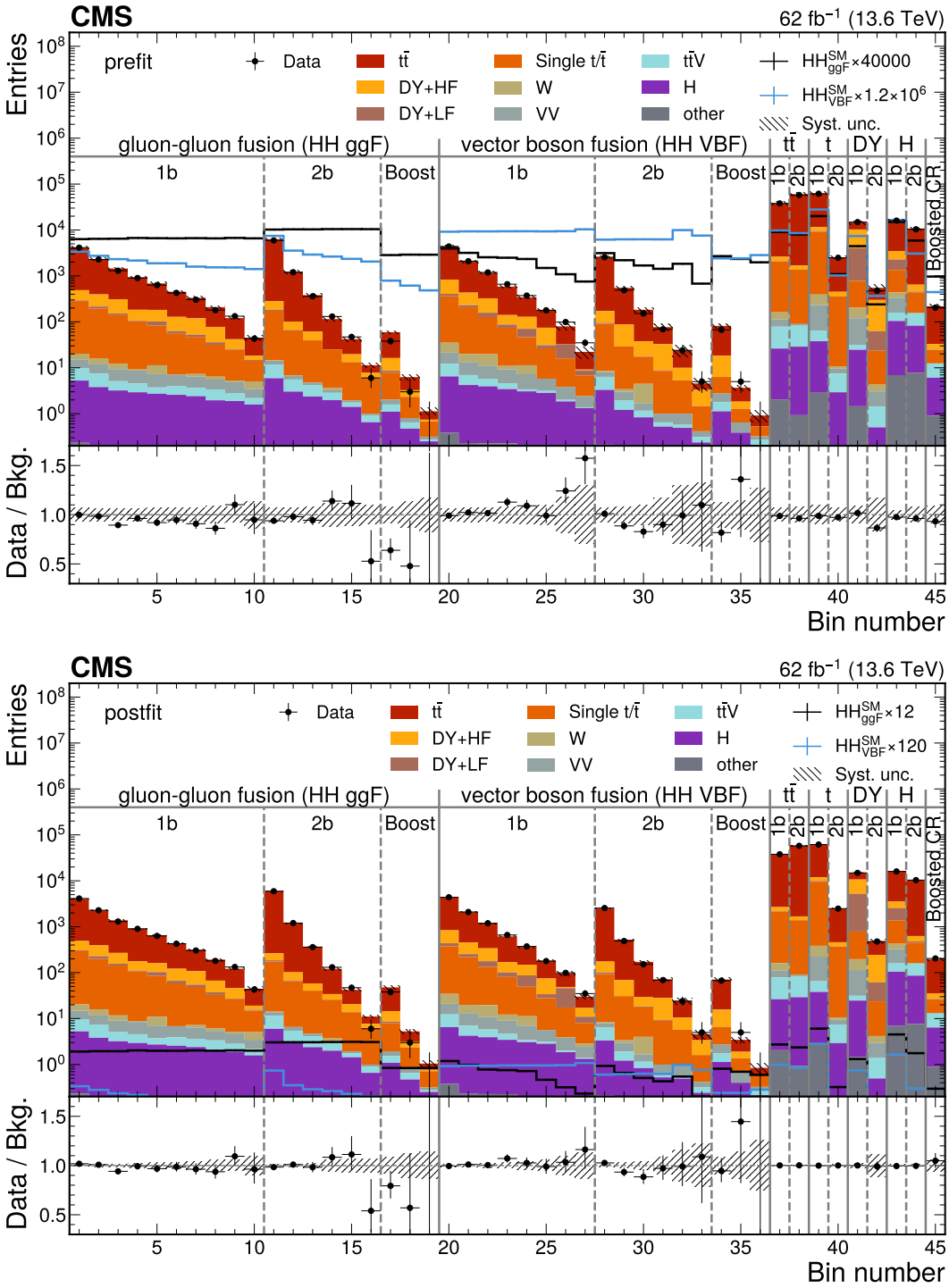


Figure 5: Observed (points) and expected (filled histograms) yields in each discriminant (NN score or category yield) bin before (upper) and after (lower) the fit to data. The HH signal distributions in the ggF and VBF production channels are overlaid (solid lines), scaled to the total background yield (top) or the observed upper limit for ggF and the observed upper limit times 10 for VBF (bottom). The uncertainty bands include the total uncertainty of the fit model. The lower panels show the ratio of the data to the expected background yields.

tion. The strong dependence of the limit on κ_{2V} is a result of the increased selection efficiency and acceptance to VBF signal events in the boosted regime for values of κ_{2V} different from 1. At $\kappa_{2V} = 1$, the signal sensitivity is equally driven by the $\geq$2b and the boosted categories, while for κ_{2V} different from 1, the sensitivity remains the same in the $\geq$2b categories but strongly improves in the boosted categories. For the results in Fig. 6, the uncertainty in the inclusive HH cross section prediction is not included in the fits but is represented as an uncertainty band on the theory prediction shown.

In Fig. 7, the observed and expected profile likelihood ratio values are presented as functions of κ_λ and κ_{2V}, where again all other couplings are assumed as in the SM. The best fit value of κ_λ is 3.4, consistent with the downward fluctuation of data in the SR_{ggF} and the minimal HH production cross section near $\kappa_\lambda = 2.5$. Values of κ_λ outside $[-9.1, 15.7]$ ($[-13.3, 19.8]$ expected) and of κ_{2V} outside $[-0.20, 2.25]$ ($[-0.48, 2.54]$ expected) are excluded at the 95% CL. The likelihood contours from a simultaneous fit of κ_λ and κ_{2V} are shown in Fig. 8. The results with statistical uncertainty only are obtained by first performing the nominal fit including systematic uncertainties, and then evaluating the likelihood with the values of the nuisance parameters used to describe the systematic uncertainties fixed to their best fit values. The background normalisation parameters are not fixed and thus contribute to the statistical uncertainties.

By far the largest source of uncertainty in the analysis arises from the limited statistical precision due to the small signal rate. The impact of the statistical uncertainties compared to the systematic effects is shown in Fig. 7.

The best fit values of the nuisance parameters used to describe the systematic uncertainties are shown in Fig. 9; they are well within one standard deviation of the prior uncertainty. The impact of each normalisation and nuisance parameter on the result is evaluated as the difference of the nominal best fit value of the HH signal strength modifier and the best fit value obtained when fixing the parameter under scrutiny to its best fit value plus/minus its postfit uncertainty. The best fit values and impacts of the 25 parameters with the highest impact are shown in Fig. 9; the nuisance parameters with the largest impact are related to the uncertainty in the inclusive HH cross section prediction (which enters the measured signal strength modifier in the denominator) and the limited size of the simulated event samples.

The results are combined with the results of the previous search with $138\,\text{fb}^{-1}$ of Run 2 data collected at $\sqrt{s} = 13\,\text{TeV}$ in final states with one or two leptons [25]. Systematic uncertainties of theoretical sources, such as cross section calculations, are treated as correlated in the combination, while experimental uncertainties, which are dominated by the uncertainties in auxiliary measurements in statistically independent data sets, are treated as uncorrelated. An observed upper limit on the HH signal strength modifier of 7.9 at 95% CL is obtained, with an expectation of 12.7.

7 Summary

A search has been presented for Higgs boson pair production in the $b\bar{b}WW$ decay channel with two leptons in the final state, conducted with $62\,\text{fb}^{-1}$ of proton-proton collision data collected at $\sqrt{s} = 13.6\,\text{TeV}$.

The data are consistent with standard model predictions. An upper limit is set on the Higgs boson pair production cross section of 12.0 times the standard model prediction at the 95% confidence level, with an expectation of 18.5. Compared to a previous search by the CMS Collaboration with $138\,\text{fb}^{-1}$ of Run 2 data collected at $\sqrt{s} = 13\,\text{TeV}$ in final states with one or

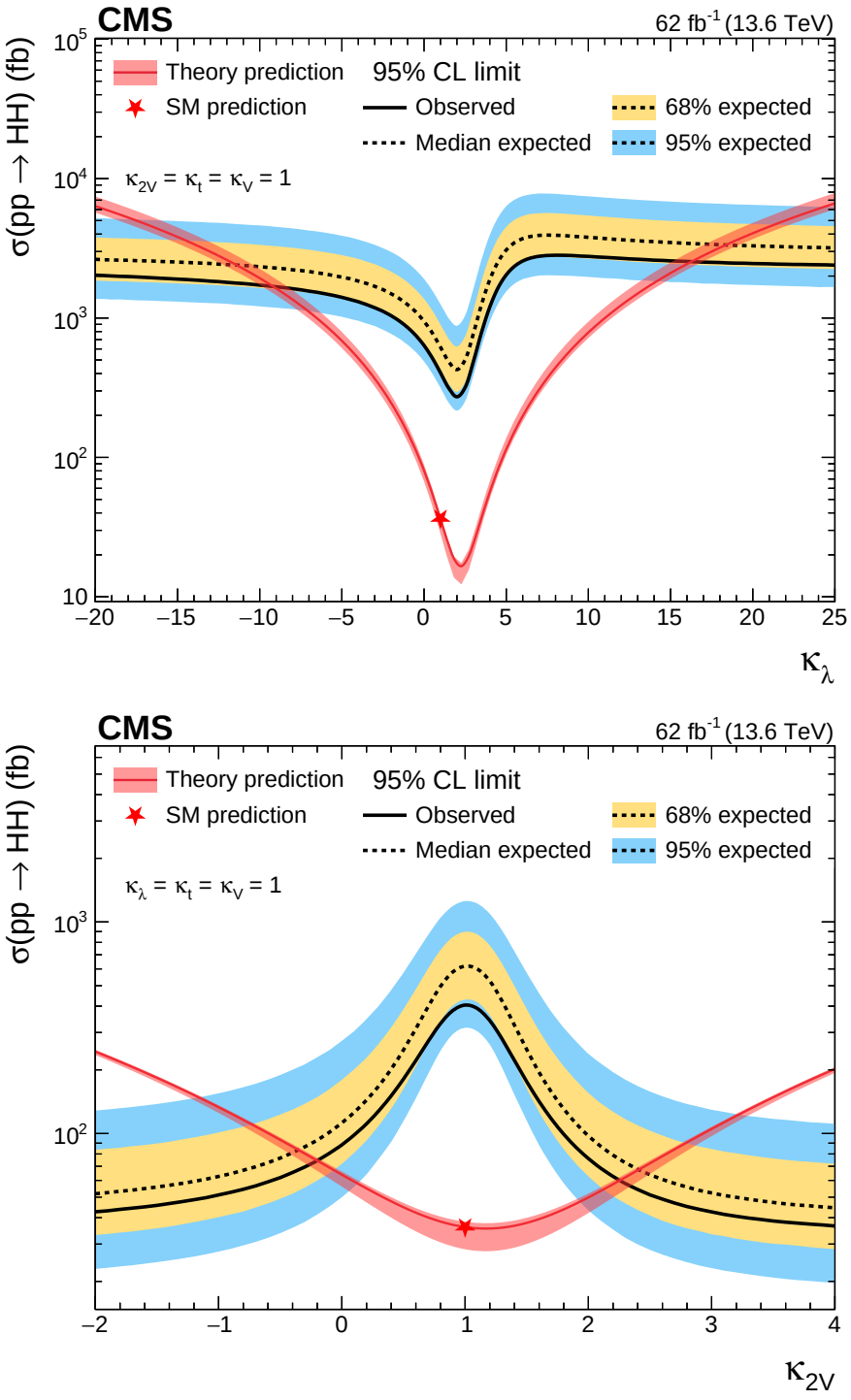


Figure 6: Observed (solid black line) and median expected (dashed black line) upper limits at the 95% CL on the inclusive HH production cross section as a function of κ_λ (upper) and κ_{2V} (lower); in both cases, all respective other couplings are fixed to the SM prediction. The yellow (blue) bands show the 68% (95%) confidence level intervals of the expected limit. The predicted cross section is overlaid (red curve), and the SM prediction is indicated (red star).

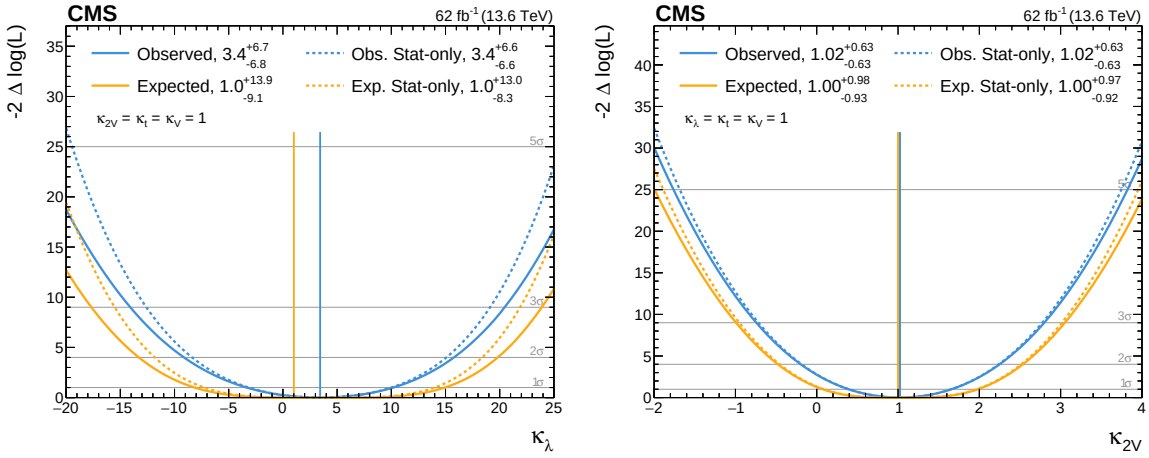


Figure 7: Observed (blue) and expected (orange) negative log-likelihood values as a function of κ_λ (left) and κ_{2V} (right), assuming all other couplings conform to the SM prediction. The solid lines include the full uncertainty model, and the dashed lines only include statistical uncertainties, which include the uncertainty components due to the $t\bar{t}$ and DY background normalisations. The vertical lines indicate the best fit value.

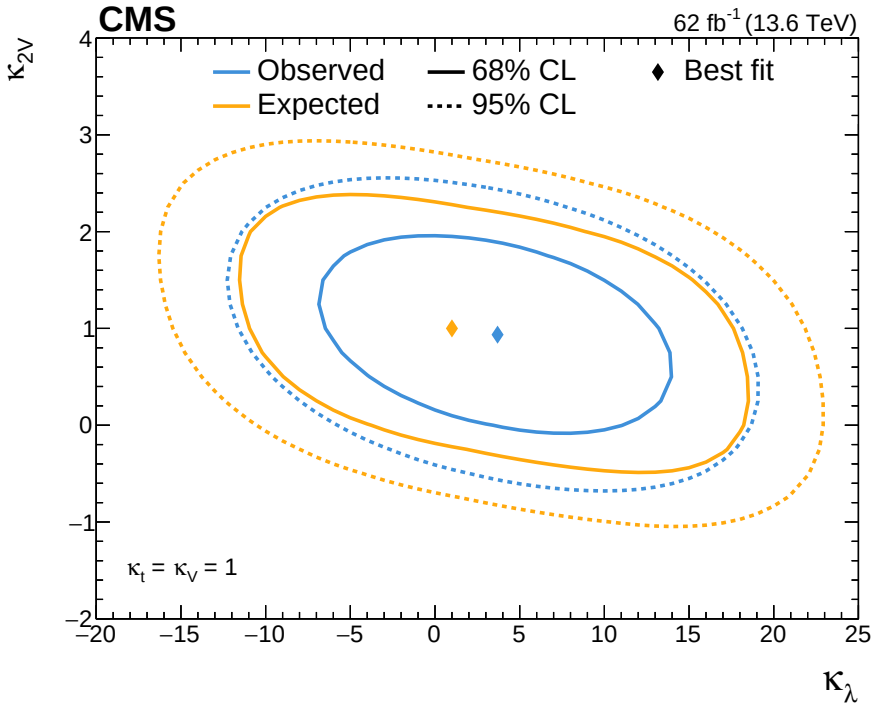


Figure 8: Observed (blue) and expected (orange) negative log-likelihood contours as a function of κ_λ and κ_{2V}, assuming all other couplings conform to the SM prediction. Shown are the best fit point (marker) and the 68% (solid lines) and 95% (dashed lines) CL contours.

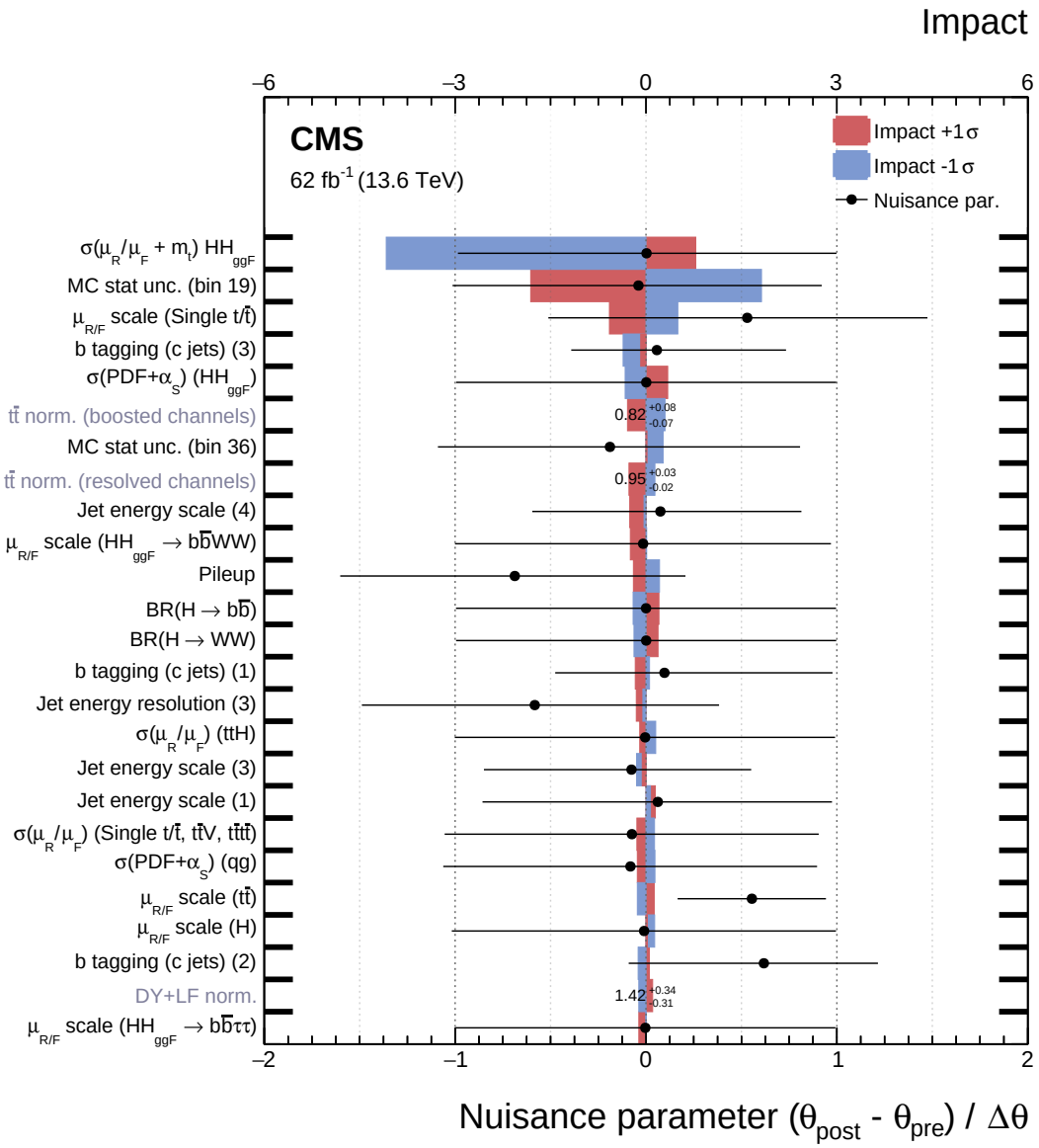


Figure 9: Best fit values of the background normalisation and nuisance parameters (black markers). The nuisance parameter values are shown as the difference of their best fit values, θ_{post}, and prefit values, θ_{pre}, relative to the prefit uncertainties $\Delta\theta$. The impact (coloured areas) of the nuisance parameters on the HH signal strength is computed as the difference of the nominal best fit value of the signal strength and the best fit value obtained when fixing the nuisance parameter under scrutiny to its best fit value θ_{post} plus/minus its postfit uncertainty. The nuisance parameters are ordered by their impact, and only the 25 highest-ranked parameters are shown. The number in parentheses for the jet energy scale and b tagging uncertainties correspond to a numbering of the data-taking period to which they are associated. The MC stat unc. refers to the systematic uncertainty due to the limited number of simulated events; in this case, the number in parentheses refers to the bin numbers shown in Fig. 5.

two leptons, the sensitivity is significantly improved through a refined classification strategy, additional triggers, and an enhanced b tagging algorithm. This yields a comparable overall expected sensitivity despite the smaller analysed data set and restriction to the two-lepton channel, with a 30% sensitivity increase in the two-lepton final state alone. The cross section limit is further used to constrain the trilinear self-coupling of the Higgs boson and the quartic coupling between two Higgs bosons and two vector bosons to $[-9.1, 15.7]$ ($[-13.3, 19.8]$ expected) and $[-0.20, 2.25]$ ($[-0.48, 2.54]$ expected) times the standard model expectation, respectively, at 95% confidence level.

The presented search is the first result on Higgs boson pair production in the $\mathrm{b\bar{b}WW}$ decay channel with $\sqrt{s} = 13.6\,\text{TeV}$ data. Combined with the results of the previous search at $\sqrt{s} = 13\,\text{TeV}$ in final states with one or two leptons, an observed upper limit is set on the Higgs boson pair production cross section of 7.9 times the standard model prediction at the 95% confidence level, with an expectation of 12.7.

Acknowledgments

We congratulate our colleagues in the CERN accelerator departments for the excellent performance of the LHC and thank the technical and administrative staffs at CERN and at other CMS institutes for their contributions to the success of the CMS effort. In addition, we gratefully acknowledge the computing centres and personnel of the Worldwide LHC Computing Grid and other centres for delivering so effectively the computing infrastructure essential to our analyses. Finally, we acknowledge the enduring support for the construction and operation of the LHC, the CMS detector, and the supporting computing infrastructure provided by the following funding agencies: SC (Armenia), BMBWF and FWF (Austria); FNRS and FWO (Belgium); CNPq, CAPES, FAPERJ, FAPERGS, and FAPESP (Brazil); MES and BNSF (Bulgaria); CERN; CAS, MoST, and NSFC (China); MINCIENCIAS (Colombia); MSES and CSF (Croatia); RIF (Cyprus); SENESCYT (Ecuador); ERC PRG and PSG, TARISTU24-TK10 and MoER TK202 (Estonia); Academy of Finland, MEC, and HIP (Finland); CEA and CNRS/IN2P3 (France); SRNSF (Georgia); BMFTR, DFG, and HGF (Germany); GSRI (Greece); NKFIH (Hungary); DAE and DST (India); IPM (Iran); SFI (Ireland); INFN (Italy); MSIT and NRF (Republic of Korea); MES (Latvia); LMTLT (Lithuania); MOE and UM (Malaysia); BUAP, CINVESTAV, CONACYT, LNS, SEP, and UASLP-FAI (Mexico); MOS (Montenegro); MBIE (New Zealand); PAEC (Pakistan); MSHE, NSC, and NAWA (Poland); FCT (Portugal); MESTD (Serbia); MICIU/AEI and PCTI (Spain); MOSTR (Sri Lanka); Swiss Funding Agencies (Switzerland); MST (Taipei); MHESI (Thailand); TUBITAK and TENMAK (Türkiye); NASU (Ukraine); STFC (United Kingdom); DOE and NSF (USA).

Individuals have received support from the Marie-Curie programme and the European Research Council and Horizon 2020 Grant, contract Nos. 675440, 724704, 752730, 758316, 765710, 824093, 101115353, 101002207, 101001205, and COST Action CA16108 (European Union); the Leventis Foundation; the Alfred P. Sloan Foundation; the Alexander von Humboldt Foundation; the Science Committee, project no. 22rl-037 (Armenia); the Fonds pour la Formation à la Recherche dans l'Industrie et dans l'Agriculture (FRIA) and Fonds voor Wetenschappelijk Onderzoek contract No. 1228724N (Belgium); the Beijing Municipal Science & Technology Commission, No. Z191100007219010, the Fundamental Research Funds for the Central Universities, the Ministry of Science and Technology of China under Grant No. 2023YFA1605804, the Natural Science Foundation of China under Grant No. 12535004, and USTC Research Funds of the Double First-Class Initiative No. YD2030002017 (China); the Ministry of Education, Youth and Sports (MEYS) of the Czech Republic; the Shota Rustaveli National Science Foundation, grant

FR-22-985 (Georgia); the Deutsche Forschungsgemeinschaft (DFG), among others, under Germany's Excellence Strategy – EXC 2121 "Quantum Universe" – 390833306, and under project number 400140256 - GRK2497; the Hellenic Foundation for Research and Innovation (HFRI), Project Number 2288 (Greece); the Hungarian Academy of Sciences, the New National Excellence Program - ÚNKP, the NKFIH research grants K 131991, K 133046, K 138136, K 143460, K 143477, K 146913, K 146914, K 147048, 2020-2.2.1-ED-2021-00181, TKP2021-NKTA-64, and 2025-1.1.5-NEMZ_KI-2025-00004 (Hungary); the Council of Science and Industrial Research, India; ICSC – National Research Centre for High Performance Computing, Big Data and Quantum Computing, FAIR – Future Artificial Intelligence Research, and CUP I53D23001070006 (Mission 4 Component 1), funded by the NextGenerationEU program, the Italian Ministry of University and Research (MUR) under Bando PRIN 2022 – CUP I53C24002390006, PRIN PRIMULA 2022RBYK7T (Italy); the Latvian Council of Science; the Ministry of Education and Science, project no. 2022/WK/14, and the National Science Centre, contracts Opus 2021/41/B/ST2/01369, 2021/43/B/ST2/01552, 2023/49/B/ST2/03273, and the NAWA contract BPN/PPO/2021/1/00011 (Poland); the Fundação para a Ciência e a Tecnologia (Portugal); the National Priorities Research Program by Qatar National Research Fund; MICIU/AEI/10.13039/501100011033, ERDF/EU, "European Union NextGenerationEU/PRTR", projects PID2022-142604OB-C21, PID2022-139519OB-C21, PID2023-147706NB-I00, PID2023-148896NB-I00, PID2023-146983NB-I00, PID2023-147115NB-I00, PID2023-148418NB-C41, PID2023-148418NB-C42, PID2023-148418NB-C43, PID2023-148418NB-C44, PID2024-158190NB-C22, RYC2021-033305-I, RYC2024-048719-I, CNS2023-144781, CNS2024-154769 and Plan de Ciencia, Tecnología e Innovación de Asturias, Spain; the Chulalongkorn Academic into Its 2nd Century Project Advancement Project, the National Science, Research and Innovation Fund program IND_FF_68_369_2300_097, and the Program Management Unit for Human Resources & Institutional Development, Research and Innovation, grant B39G680009 (Thailand); the Eric & Wendy Schmidt Fund for Strategic Innovation through the CERN Next Generation Triggers project under grant agreement number SIF-2023-004; the Kavli Foundation; the Nvidia Corporation; the SuperMicro Corporation; the Welch Foundation, contract C-1845; and the Weston Havens Foundation (USA).

References

[1] ATLAS Collaboration, "Observation of a new particle in the search for the standard model Higgs boson with the ATLAS detector at the LHC", *Phys. Lett. B* **716** (2012) 1, doi:10.1016/j.physletb.2012.08.020, arXiv:1207.7214.

[2] CMS Collaboration, "Observation of a new boson at a mass of 125 GeV with the CMS experiment at the LHC", *Phys. Lett. B* **716** (2012) 30, doi:10.1016/j.physletb.2012.08.021, arXiv:1207.7235.

[3] CMS Collaboration, "Observation of a new boson with mass near 125 GeV in pp collisions at $\sqrt{s} = 7$ and 8 TeV", *JHEP* **06** (2013) 081, doi:10.1007/JHEP06(2013)081, arXiv:1303.4571.

[4] F. Englert and R. Brout, "Broken symmetry and the mass of gauge vector mesons", *Phys. Rev. Lett.* **13** (1964) 321, doi:10.1103/PhysRevLett.13.321.

[5] P. W. Higgs, "Broken symmetries, massless particles and gauge fields", *Phys. Lett.* **12** (1964) 132, doi:10.1016/0031-9163(64)91136-9.

[6] P. W. Higgs, "Broken symmetries and the masses of gauge bosons", *Phys. Rev. Lett.* **13** (1964) 508, doi:10.1103/PhysRevLett.13.508.

[7] G. S. Guralnik, C. R. Hagen, and T. W. B. Kibble, "Global conservation laws and massless particles", *Phys. Rev. Lett.* **13** (1964) 585, doi:10.1103/PhysRevLett.13.585.

[8] P. W. Higgs, "Spontaneous symmetry breakdown without massless bosons", *Phys. Rev.* **145** (1966) 1156, doi:10.1103/PhysRev.145.1156.

[9] T. W. B. Kibble, "Symmetry breaking in non-Abelian gauge theories", *Phys. Rev.* **155** (1967) 1554, doi:10.1103/PhysRev.155.1554.

[10] S. Weinberg, "A model of leptons", *Phys. Rev. Lett.* **19** (1967) 1264, doi:10.1103/PhysRevLett.19.1264.

[11] A. Salam, "Weak and electromagnetic interactions", *Conf. Proc. C* **680519** (1968) 367, doi:10.1142/9789812795915_0034.

[12] ATLAS Collaboration, "A detailed map of Higgs boson interactions by the ATLAS experiment ten years after the discovery", *Nature* **607** (2022) 52, doi:10.1038/s41586-022-04893-w, arXiv:2207.00092. [Erratum: doi:10.1038/s41586-022-05581-5].

[13] CMS Collaboration, "A portrait of the Higgs boson by the CMS experiment ten years after the discovery", *Nature* **607** (2022) 60, doi:10.1038/s41586-022-04892-x, arXiv:2207.00043. [Corrigendum: doi:10.1038/s41586-023-06164-8].

[14] G. Heinrich et al., "Probing the trilinear Higgs boson coupling in di-Higgs production at NLO QCD including parton shower effects", *JHEP* **06** (2019) 066, doi:10.1007/JHEP06(2019)066, arXiv:1903.08137.

[15] M. Grazzini et al., "Higgs boson pair production at NNLO with top quark mass effects", *JHEP* **05** (2018) 059, doi:10.1007/JHEP05(2018)059, arXiv:1803.02463.

[16] A. Karlberg et al., "Ad interim recommendations for the Higgs boson production cross sections at $\sqrt{s} = 13.6\,\text{TeV}$", 2024. arXiv:2402.09955.

[17] J. Baglio et al., "gg $\to$ HH: Combined uncertainties", *Phys. Rev. D* **103** (2021) 056002, doi:10.1103/PhysRevD.103.056002, arXiv:2008.11626.

[18] F. A. Dreyer, A. Karlberg, J.-N. Lang, and M. Pellen, "Precise predictions for double-Higgs production via vector-boson fusion", *Eur. Phys. J. C* **80** (2020) 1037, doi:10.1140/epjc/s10052-020-08610-7, arXiv:2005.13341.

[19] F. A. Dreyer and A. Karlberg, "Vector-boson fusion Higgs pair production at N^{3}LO", *Phys. Rev. D* **98** (2018) 114016, doi:10.1103/PhysRevD.98.114016, arXiv:1811.07906.

[20] F. Bishara, R. Contino, and J. Rojo, "Higgs pair production in vector-boson fusion at the LHC and beyond", *Eur. Phys. J. C* **77** (2017) 481, doi:10.1140/epjc/s10052-017-5037-9, arXiv:1611.03860.

[21] ATLAS Collaboration, "Combination of searches for Higgs boson pair production in pp collisions at $\sqrt{s} = 13\,\text{TeV}$ with the ATLAS detector", *Phys. Rev. Lett.* **133** (2024) 101801, doi:10.1103/PhysRevLett.133.101801, arXiv:2406.09971.

[22] CMS Collaboration, "Combination of searches for nonresonant Higgs boson pair production in proton-proton collisions at $\sqrt{s} = 13\,\text{TeV}$", 2025. arXiv:2510.07527. Submitted to Reports on Progress in Physics.

[23] ATLAS and CMS Collaborations, "Combination of ATLAS and CMS searches for Higgs boson pair production at $\sqrt{s} = 13\,\text{TeV}$", 2026. arXiv:2602.23991. Submitted to Physics Review Letters.

[24] ATLAS Collaboration, "Study of Higgs boson pair production in the $HH \to b\bar{b}\gamma\gamma$ final state with $308\,\text{fb}^{-1}$ of data collected at $\sqrt{s} = 13\,\text{TeV}$ and 13.6 TeV by the ATLAS experiment", 2025. arXiv:2507.03495. Submitted to Phys. Lett. B.

[25] CMS Collaboration, "Search for Higgs boson pair production in the $\text{b}\bar{\text{b}}\text{W}^+\text{W}^-$ decay mode in proton-proton collisions at $\sqrt{s} = 13$ TeV", *JHEP* **07** (2024) 293, doi:10.1007/JHEP07(2024)293, arXiv:2403.09430.

[26] ATLAS Collaboration, "Search for non-resonant Higgs boson pair production in the $2b + 2\ell + E_{\text{T}}^{\text{miss}}$ final state in pp collisions at $\sqrt{s} = 13\,\text{TeV}$ with the ATLAS detector", *JHEP* **02** (2024) 037, doi:10.1007/JHEP02(2024)037, arXiv:2310.11286.

[27] LHC Higgs Cross Section Working Group, "Handbook of LHC Higgs cross sections: 3. Higgs properties", 2013. arXiv:1307.1347.

[28] HEPData record for this analysis, 2026. doi:10.17182/hepdata.168471.

[29] CMS Collaboration, "The CMS experiment at the CERN LHC", *JINST* **3** (2008) S08004, doi:10.1088/1748-0221/3/08/S08004.

[30] CMS Collaboration, "Development of the CMS detector for the CERN LHC Run 3", *JINST* **19** (2024) P05064, doi:10.1088/1748-0221/19/05/P05064, arXiv:2309.05466.

[31] CMS Collaboration, "Performance of the CMS level-1 trigger in proton-proton collisions at $\sqrt{s} = 13\,\text{TeV}$", *JINST* **15** (2020) P10017, doi:10.1088/1748-0221/15/10/P10017, arXiv:2006.10165.

[32] CMS Collaboration, "The CMS trigger system", *JINST* **12** (2017) P01020, doi:10.1088/1748-0221/12/01/P01020, arXiv:1609.02366.

[33] CMS Collaboration, "Performance of the CMS high-level trigger during LHC Run 2", *JINST* **19** (2024) P11021, doi:10.1088/1748-0221/19/11/P11021, arXiv:2410.17038.

[34] CMS Collaboration, "Electron and photon reconstruction and identification with the CMS experiment at the CERN LHC", *JINST* **16** (2021) P05014, doi:10.1088/1748-0221/16/05/P05014, arXiv:2012.06888.

[35] CMS Collaboration, "Performance of the CMS muon detector and muon reconstruction with proton-proton collisions at $\sqrt{s} = 13\,\text{TeV}$", *JINST* **13** (2018) P06015, doi:10.1088/1748-0221/13/06/P06015, arXiv:1804.04528.

[36] CMS Collaboration, "Description and performance of track and primary-vertex reconstruction with the CMS tracker", *JINST* **9** (2014) P10009, doi:10.1088/1748-0221/9/10/P10009, arXiv:1405.6569.

[37] CMS Collaboration, "Particle-flow reconstruction and global event description with the CMS detector", *JINST* **12** (2017) P10003, doi:10.1088/1748-0221/12/10/P10003, arXiv:1706.04965.

[38] CMS Collaboration, "Jet energy scale and resolution in the CMS experiment in pp collisions at 8 TeV", *JINST* **12** (2017) P02014, doi:10.1088/1748-0221/12/02/P02014, arXiv:1607.03663.

[39] CMS Collaboration, "Performance of missing transverse momentum reconstruction in proton-proton collisions at $\sqrt{s} = 13$ TeV using the CMS detector", *JINST* **14** (2019) P07004, doi:10.1088/1748-0221/14/07/P07004, arXiv:1903.06078.

[40] CMS Collaboration, "ECAL 2016 refined calibration and Run 2 summary plots", CMS Detector Performance Summary CMS-DP-2020-021, https://cds.cern.ch/record/2717925, 2020.

[41] CMS Collaboration, "Pileup mitigation at CMS in 13 TeV data", *JINST* **15** (2020) P09018, doi:10.1088/1748-0221/15/09/p09018, arXiv:2003.00503.

[42] M. Cacciari, G. P. Salam, and G. Soyez, "The anti-k_{T} jet clustering algorithm", *JHEP* **04** (2008) 063, doi:10.1088/1126-6708/2008/04/063, arXiv:0802.1189.

[43] M. Cacciari, G. P. Salam, and G. Soyez, "FastJet user manual", *Eur. Phys. J. C* **72** (2012) 1896, doi:10.1140/epjc/s10052-012-1896-2, arXiv:1111.6097.

[44] D. Bertolini, P. Harris, M. Low, and N. Tran, "Pileup per particle identification", *JHEP* **10** (2014) 059, doi:10.1007/JHEP10(2014)059, arXiv:1407.6013.

[45] H. Qu and L. Gouskos, "ParticleNet: Jet tagging via particle clouds", *Phys. Rev. D* **101** (2020) 056019, doi:10.1103/PhysRevD.101.056019, arXiv:1902.08570.

[46] CMS Collaboration, "Run 3 commissioning results of heavy-flavor jet tagging at $\sqrt{s} = 13.6$ TeV with CMS data using a modern framework for data processing", CMS Detector Performance Summary CMS-DP-2024-024, https://cds.cern.ch/record/2898463, 2024.

[47] CMS Collaboration, "A unified approach for jet tagging in Run 3 at $\sqrt{s} = 13.6$ TeV in CMS", CMS Detector Performance Summary CMS-DP-2024-066, 2024.

[48] CMS Collaboration, "Performance of heavy-flavour jet identification in Lorentz-boosted topologies in proton-proton collisions at $\sqrt{s} = 13$ TeV", *JINST* **20** (2025) P11006, doi:10.1088/1748-0221/20/11/P11006, arXiv:2510.10228.

[49] CMS Collaboration, "Identification of heavy-flavour jets with the CMS detector in pp collisions at 13 TeV", *JINST* **13** (2018) P05011, doi:10.1088/1748-0221/13/05/P05011, arXiv:1712.07158.

[50] CMS Collaboration, "Performance summary of AK4 jet b tagging with data from 2022 proton-proton collisions at $\sqrt{s} = 13.6$ TeV with the CMS detector", CMS Detector Performance Summary CMS-DP-2024-025, https://cds.cern.ch/record/2898464, 2024.

[51] P. Nason, "A new method for combining NLO QCD with shower Monte Carlo algorithms", *JHEP* **11** (2004) 040, doi:10.1088/1126-6708/2004/11/040, arXiv:hep-ph/0409146.

[52] S. Frixione, P. Nason, and C. Oleari, "Matching NLO QCD computations with parton shower simulations: The POWHEG method", *JHEP* **11** (2007) 070, doi:10.1088/1126-6708/2007/11/070, arXiv:0709.2092.

[53] S. Alioli, P. Nason, C. Oleari, and E. Re, "A general framework for implementing NLO calculations in shower Monte Carlo programs: The POWHEG BOX", *JHEP* **06** (2010) 043, doi:10.1007/JHEP06(2010)043, arXiv:1002.2581.

[54] T. Ježo and P. Nason, "On the treatment of resonances in next-to-leading order calculations matched to a parton shower", *JHEP* **12** (2015) 065, doi:10.1007/JHEP12(2015)065, arXiv:1509.09071.

[55] J. Alwall et al., "The automated computation of tree-level and next-to-leading order differential cross sections, and their matching to parton shower simulations", *JHEP* **07** (2014) 079, doi:10.1007/JHEP07(2014)079, arXiv:1405.0301.

[56] GEANT4 Collaboration, "GEANT4—a simulation toolkit", *Nucl. Instrum. Meth. A* **506** (2003) 250, doi:10.1016/S0168-9002(03)01368-8.

[57] NNPDF Collaboration, "Parton distributions from high-precision collider data", *Eur. Phys. J. C* **77** (2017) 663, doi:10.1140/epjc/s10052-017-5199-5, arXiv:1706.00428.

[58] C. Bierlich et al., "A comprehensive guide to the physics and usage of PYTHIA 8.3", *SciPost Phys. Codeb.* **2022** (2022) 8, doi:10.21468/SciPostPhysCodeb.8, arXiv:2203.11601.

[59] CMS Collaboration, "Extraction and validation of a new set of CMS PYTHIA 8 tunes from underlying-event measurements", *Eur. Phys. J. C* **80** (2020) 4, doi:10.1140/epjc/s10052-019-7499-4, arXiv:1903.12179.

[60] E. Bagnaschi, G. Degrassi, P. Slavich, and A. Vicini, "Higgs production via gluon fusion in the POWHEG approach in the SM and in the MSSM", *JHEP* **02** (2012) 088, doi:10.1007/JHEP02(2012)088, arXiv:1111.2854.

[61] G. Heinrich et al., "NLO predictions for Higgs boson pair production with full top quark mass dependence matched to parton showers", *JHEP* **08** (2017) 088, doi:10.1007/JHEP08(2017)088, arXiv:1703.09252.

[62] S. Frixione, P. Nason, and G. Ridolfi, "A positive-weight next-to-leading-order Monte Carlo for heavy flavour hadroproduction", *JHEP* **09** (2007) 126, doi:10.1088/1126-6708/2007/09/126, arXiv:0707.3088.

[63] CMS Collaboration, "Measurement of differential cross sections for the production of top quark pairs and of additional jets in lepton+jets events from pp collisions at $\sqrt{s} = 13\,\text{TeV}$", *Phys. Rev. D* **97** (2018) 112003, doi:10.1103/PhysRevD.97.112003, arXiv:1803.08856.

[64] CMS Collaboration, "Differential cross section measurements for the production of top quark pairs and of additional jets using dilepton events from pp collisions at $\sqrt{s} = 13\,\text{TeV}$", *JHEP* **02** (2025) 064, doi:10.1007/JHEP02(2025)064, arXiv:2402.08486.

[65] M. Czakon et al., "Top-pair production at the LHC through NNLO QCD and NLO EW", *JHEP* **10** (2017) 186, doi:10.1007/JHEP10(2017)186, arXiv:1705.04105.

[66] CMS Collaboration, "Measurement of inclusive and differential cross sections of single top quark production in association with a W boson in proton-proton collisions at $\sqrt{s} = 13.6$ TeV", *JHEP* **01** (2025) 107, doi:10.1007/JHEP01(2025)107, arXiv:2409.06444.

[67] M. Beneke, P. Falgari, S. Klein, and C. Schwinn, "Hadronic top-quark pair production with NNLL threshold resummation", *Nucl. Phys. B* **855** (2012) 695, doi:10.1016/j.nuclphysb.2011.10.021, arXiv:1109.1536.

[68] M. Cacciari et al., "Top-pair production at hadron colliders with next-to-next-to-leading logarithmic soft-gluon resummation", *Phys. Lett. B* **710** (2012) 612, doi:10.1016/j.physletb.2012.03.013, arXiv:1111.5869.

[69] P. Bärnreuther, M. Czakon, and A. Mitov, "Percent-level-precision physics at the Tevatron: Next-to-next-to-leading order QCD corrections to $q\bar{q} \to t\bar{t}$+X", *Phys. Rev. Lett.* **109** (2012) 132001, doi:10.1103/PhysRevLett.109.132001, arXiv:1204.5201.

[70] M. Czakon and A. Mitov, "NNLO corrections to top-pair production at hadron colliders: The all-fermionic scattering channels", *JHEP* **12** (2012) 054, doi:10.1007/JHEP12(2012)054, arXiv:1207.0236.

[71] M. Czakon and A. Mitov, "NNLO corrections to top pair production at hadron colliders: The quark-gluon reaction", *JHEP* **01** (2013) 080, doi:10.1007/JHEP01(2013)080, arXiv:1210.6832.

[72] M. Czakon, P. Fiedler, and A. Mitov, "Total top-quark pair-production cross section at hadron colliders through $\mathcal{O}(\alpha_s^4)$", *Phys. Rev. Lett.* **110** (2013) 252004, doi:10.1103/PhysRevLett.110.252004, arXiv:1303.6254.

[73] M. Czakon and A. Mitov, "Top++: A program for the calculation of the top-pair cross-section at hadron colliders", *Comput. Phys. Commun.* **185** (2014) 2930, doi:10.1016/j.cpc.2014.06.021, arXiv:1112.5675.

[74] S. Alioli, P. Nason, C. Oleari, and E. Re, "NLO single-top production matched with shower in POWHEG: s- and t-channel contributions", *JHEP* **09** (2009) 111, doi:10.1088/1126-6708/2009/09/111, arXiv:0907.4076. [Erratum: doi:10.1007/JHEP02(2010)011].

[75] E. Re, "Single-top Wt-channel production matched with parton showers using the POWHEG method", *Eur. Phys. J. C* **71** (2011) 1547, doi:10.1140/epjc/s10052-011-1547-z, arXiv:1009.2450.

[76] N. Kidonakis, "Two-loop soft anomalous dimensions for single top quark associated production with W^- or H^-", *Phys. Rev. D* **82** (2010) 054018, doi:10.1103/PhysRevD.82.054018, arXiv:1005.4451.

[77] M. Aliev et al., "HATHOR: HAdronic Top and Heavy quarks crOss section calculatoR", *Comput. Phys. Commun.* **182** (2011) 1034, doi:10.1016/j.cpc.2010.12.040, arXiv:1007.1327.

[78] P. Kant et al., "HatHor for single top-quark production: Updated predictions and uncertainty estimates for single top-quark production in hadronic collisions", *Comput. Phys. Commun.* **191** (2015) 74, doi:10.1016/j.cpc.2015.02.001, arXiv:1406.4403.

[79] R. Frederix and S. Frixione, "Merging meets matching in MC@NLO", *JHEP* **12** (2012) 061, doi:10.1007/JHEP12(2012)061, arXiv:1209.6215.

[80] S. Alioli, P. Nason, C. Oleari, and E. Re, "NLO Higgs boson production via gluon fusion matched with shower in POWHEG", *JHEP* **04** (2009) 002, doi:10.1088/1126-6708/2009/04/002, arXiv:0812.0578.

[81] P. Nason and C. Oleari, "NLO Higgs boson production via vector-boson fusion matched with shower in POWHEG", *JHEP* **02** (2010) 037, doi:10.1007/JHEP02(2010)037, arXiv:0911.5299.

[82] K. Mimasu, V. Sanz, and C. Williams, "Higher order QCD predictions for associated Higgs production with anomalous couplings to gauge bosons", *JHEP* **08** (2016) 039, doi:10.1007/JHEP08(2016)039, arXiv:1512.02572.

[83] S. P. Jones, M. Kerner, and G. Luisoni, "Next-to-leading-order QCD corrections to Higgs boson plus jet production with full top-quark mass dependence", *Phys. Rev. Lett.* **120** (2018) 162001, doi:10.1103/PhysRevLett.120.162001, arXiv:1802.00349. [Erratum: doi:10.1103/PhysRevLett.128.059901].

[84] H. B. Hartanto, B. Jager, L. Reina, and D. Wackeroth, "Higgs boson production in association with top quarks in the POWHEG BOX", *Phys. Rev. D* **91** (2015) 094003, doi:10.1103/PhysRevD.91.094003, arXiv:1501.04498.

[85] P. Nason and G. Zanderighi, "W^+W^- , WZ and ZZ production in the POWHEG-BOX-V2", *Eur. Phys. J. C* **74** (2014) 2702, doi:10.1140/epjc/s10052-013-2702-5, arXiv:1311.1365.

[86] M. Erdmann, J. Glombitza, G. Kasieczka, and U. Klemradt, "Deep Learning for Physics Research". World Scientific, 2021. doi:10.1142/12294.

[87] A. Ghorbani and J. Zou, "Data Shapley: Equitable valuation of data for machine learning", 2019. arXiv:1904.02868.

[88] M. Cacciari et al., "The $t\bar{t}$ cross-section at 1.8 TeV and 1.96 TeV: A study of the systematics due to parton densities and scale dependence", *JHEP* **04** (2004) 068, doi:10.1088/1126-6708/2004/04/068, arXiv:hep-ph/0303085.

[89] PDF4LHC Working Group Collaboration, "The PDF4LHC21 combination of global PDF fits for the LHC Run III", *J. Phys. G* **49** (2022) 080501, doi:10.1088/1361-6471/ac7216, arXiv:2203.05506.

[90] CMS Collaboration, "Luminosity measurement in proton-proton collisions at 13.6 TeV in 2022 at CMS", CMS Physics Analysis Summary CMS-PAS-LUM-22-001, https://cds.cern.ch/record/2890833, 2024.

[91] CMS Collaboration, "Measurement of the offline integrated luminosity for the CMS proton-proton collision dataset recorded in 2023", CMS Detector Performance Summary CMS-DP-2024-068, https://cds.cern.ch/record/2904808, 2024.

[92] J. S. Conway, "Incorporating nuisance parameters in likelihoods for multisource spectra", in *Proc. Workshop on statistical issues related to discovery claims in search experiments and unfolding*, p. 115. 2011. arXiv:1103.0354. doi:10.5170/CERN-2011-006.115.

[93] CMS Collaboration, "The CMS statistical analysis and combination tool: COMBINE", *Comput. Softw. Big Sci.* **8** (2024) 19, doi:10.1007/s41781-024-00121-4, arXiv:2404.06614.

[94] CMS Collaboration, "First measurement of the top quark pair production cross section in proton-proton collisions at $\sqrt{s} = 13.6\,\text{TeV}$", *JHEP* **08** (2023) 204, doi:10.1007/JHEP08(2023)204, arXiv:2303.10680.

[95] T. Junk, "Confidence level computation for combining searches with small statistics", *Nucl. Instrum. Meth. A* **434** (1999) 435, doi:10.1016/S0168-9002(99)00498-2, arXiv:hep-ex/9902006.

[96] A. L. Read, "Presentation of search results: The CL_s technique", *J. Phys. G* **28** (2002) 2693, doi:10.1088/0954-3899/28/10/313.

[97] G. Cowan, K. Cranmer, E. Gross, and O. Vitells, "Asymptotic formulae for likelihood-based tests of new physics", *Eur. Phys. J. C* **71** (2011) 1554, doi:10.1140/epjc/s10052-011-1554-0, arXiv:1007.1727. [Erratum: doi:10.1140/epjc/s10052-013-2501-z].

A The CMS Collaboration

Yerevan Physics Institute, Yerevan, Armenia
A. Gevorgyan, A. Hayrapetyan, V. Makarenko, A. Tumasyan[1]

Marietta Blau Institute for Particle Physics, Vienna, Austria
W. Adam, L. Benato, T. Bergauer, M. Dragicevic, S. Gundacker, A.K. Guven, P.S. Hussain, M. Jeitler[2], N. Krammer, A. Li, D. Liko, M. Matthewman, J. Schieck[2], R. Schöfbeck[2], M. Shooshtari, M. Sonawane, N. Van Den Bossche, W. Waltenberger, C.-E. Wulz[2]

Universiteit Antwerpen, Antwerpen, Belgium
T. Janssen, D. Ocampo Henao, T. Van Laer, P. Van Mechelen

Vrije Universiteit Brussel, Brussel, Belgium
D. Ahmadi, J. Bierkens, N. Breugelmans, S. Dansana, A. De Moor, M. Delcourt, S. Duponcheel, C. Gupta, F. Heyen, Y. Hong, K. Kang, P. Kashko, S. Lowette, I. Makarenko, S. Nandakumar, S. Tavernier, M. Tytgat[3], G.P. Van Onsem, S. Van Putte, T. Wybouw

Université Libre de Bruxelles, Bruxelles, Belgium
A. Beshr, B. Bilin, F. Caviglia Roman, B. Clerbaux, A.K. Das, I. De Bruyn, G. De Lentdecker, E. Ducarme, H. Evard, L. Favart, I. Kalaitzidou, A. Khalilzadeh, A. Malara, M.A. Shahzad, L. Thomas, M. Vanden Bemden, C. Vander Velde, P. Vanlaer, C. Yuan, F. Zhang

Ghent University, Ghent, Belgium
A. Cauwels, M. De Coen, D. Dobur, C. Giordano, G. Gokbulut, K. Kaspar, D. Kavtaradze, D. Marckx, A. Mehta, K. Skovpen, A.M. Tomaru, J. van der Linden, J. Vandenbroeck

Université Catholique de Louvain, Louvain-la-Neuve, Belgium
H. Aarup Petersen, A. Benecke, A. Bethani, A. Cappati, J. De Favereau De Jeneret, C. Delaere, F. Gameiro Casalinho, A. Giammanco, A.O. Guzel, M. Hussain, Z. Lawrence, J. Lidrych, P. Malek, S. Turkcapar

Centro Brasileiro de Pesquisas Fisicas, Rio de Janeiro, Brazil
G.A. Alves, M. Barroso Ferreira Filho, E. Coelho, M.V. Gonçalves Sales, C. Hensel, D. Matos Figueiredo, T. Menezes De Oliveira, C. Mora Herrera, P. Rebello Teles, M. Soeiro, E.J. Tonelli Manganote[4], A. Vilela Pereira

Universidade do Estado do Rio de Janeiro, Rio de Janeiro, Brazil
W.L. Aldá Júnior, H. Brandao Malbouisson, W. Carvalho, J. Chinellato[5], G. Correia Silva, M. Costa Reis, E.M. Da Costa, D. Da Silva Dalto, G.G. Da Silveira[6], D. De Jesus Damiao, S. Fonseca De Souza, R. Gomes De Souza, S. S. Jesus, T. Laux Kuhn[6], K. Maslova, K. Mota Amarilo, L. Mundim, H. Nogima, J.P. Pinheiro, A. Santoro, A. Sznajder, M. Thiel, F. Torres Da Silva De Araujo[7], D. Torres Machado

Universidade Estadual Paulista, Universidade Federal do ABC, São Paulo, Brazil
C.A. Bernardes, L. Calligaris, J. Carvalho Leite, M. P. Coelho, F. Damas, T.R. Fernandez Perez Tomei, E.M. Gregores, B. Lopes Da Costa, I. Maietto Silverio, P.G. Mercadante, S.F. Novaes, Sandra S. Padula, V. Scheurer

Institute for Nuclear Research and Nuclear Energy, Bulgarian Academy of Sciences, Sofia,

Bulgaria
A. Aleksandrov, G. Antchev, P. Danev, R. Hadjiiska, P. Iaydjiev, M. Shopova, G. Sultanov

University of Sofia, Sofia, Bulgaria
A. Dimitrov, L. Litov, B. Pavlov, P. Petkov, A. Petrov

Instituto De Alta Investigación, Universidad de Tarapacá, Casilla 7 D, Arica, Chile
S. Keshri, D. Laroze, M. Meena, S. Thakur

Universidad Tecnica Federico Santa Maria, Valparaiso, Chile
W. Brooks

Beihang University, Beijing, China
T. Cheng, L. Wang, L. Yuan

Department of Physics, Tsinghua University, Beijing, China
J. Gu, Z. Hu, Z. Liang, J. Liu, X. Wang, Y. Wang, H. Yang, S. Zhang, Y. Zhao

Institute of High Energy Physics, Beijing, China
N. Bi[8], G.M. Chen[8], H.S. Chen[8], M. Chen[8], Y. Chen, B. Hou[8], Q. Hou, F. Iemmi, C.H. Jiang, P.z. Lai, H. Liao, G. Liu, Z.-A. Liu[9], S. Song[8], J. Tao, C. Wang[8], J. Wang, A. Zada[8], H. Zhang, J. Zhao

State Key Laboratory of Nuclear Physics and Technology, Peking University, Beijing, China
Y. Ban, A. Carvalho Antunes De Oliveira, S. Deng, X. Geng, B. Guo, Q. Guo, Z. He, C. Jiang, A. Levin, C. Li, L. Li, Q. Li, Y. Mao, S. Qian, S.J. Qian, X. Qin, C. Quaranta, X. Sun, D. Wang, J. Wang, T. Yang, M. Zhang, M. Zhang, Y. Zhao, C. Zhou

State Key Laboratory of Nuclear Physics and Technology, Institute of Quantum Matter, South China Normal University, Guangzhou, China
X. Hua, S. Yang

Sun Yat-Sen University, Guangzhou, China
Z. You

University of Science and Technology of China, Hefei, China
N. Lu

Nanjing Normal University, Nanjing, China
G. Bauer[10,11], L. Chen, Z. Cui[11], B. Li[12], H. Wang, K. Yi[13], J. Zhang, F. Zhu

Institute of Frontier and Interdisciplinary Science, Shandong University, Qingdao, China
C. Li

Institute of Modern Physics and Key Laboratory of Nuclear Physics and Ion-beam Application (MOE) - Fudan University, Shanghai, China
Y. Li, Z. Wang, Y. Zhou[14]

Zhejiang University, Hangzhou, Zhejiang, China
Z. Lin, C. Lu, M. Xiao[15]

Universidad de Los Andes, Bogota, Colombia
C. Avila, A. Cabrera, C. Florez, J.A. Reyes Vega

Universidad de Antioquia, Medellin, Colombia

C. Rendón, M. Rodriguez, A.A. Ruales Barbosa, J.D. Ruiz Alvarez

University of Split, Faculty of Electrical Engineering, Mechanical Engineering and Naval Architecture, Split, Croatia
N. Godinovic, D. Lelas, I. Puljak, A. Sculac

University of Split, Faculty of Science, Split, Croatia
M. Kovac, A. Petkovic, T. Sculac

Institute Rudjer Boskovic, Zagreb, Croatia
P. Bargassa, V. Brigljevic, D. Ferencek, K. Jakovcic, A. Starodumov, T. Susa

University of Cyprus, Nicosia, Cyprus
A. Attikis, S. Konstantinou, C. Leonidou, L. Paizanos, F. Ptochos, P.A. Razis, H. Saka, A. Stepennov

Charles University, Prague, Czech Republic
M. Finger[†], M. Finger Jr.

Escuela Politecnica Nacional, Quito, Ecuador
E. Acurio

Universidad San Francisco de Quito, Quito, Ecuador
E. Carrera Jarrin

Academy of Scientific Research and Technology of the Arab Republic of Egypt, Egyptian Network of High Energy Physics, Cairo, Egypt
A.A. Abdelalim[16,17], B. El-mahdy[18]

Center for High Energy Physics (CHEP-FU), Fayoum University, El-Fayoum, Egypt
A. Hussein, M.A. Mahmoud, H. Mohammed

National Institute of Chemical Physics and Biophysics, Tallinn, Estonia
K. Jaffel, M. Kadastik, T. Lange, C. Nielsen, J. Pata, M. Raidal, N. Seeba, L. Tani

Department of Physics, University of Helsinki, Helsinki, Finland
E. Brücken, A. Milieva, K. Osterberg, M. Voutilainen

Helsinki Institute of Physics, Helsinki, Finland
F. Garcia, T. Hilden, P. Inkaew, K.T.S. Kallonen, R. Kumar Verma, T. Lampén, K. Lassila-Perini, B. Lehtela, S. Lehti, T. Lindén, N.R. Mancilla Xinto, M. Myllymäki, M.m. Rantanen, S. Saariokari, N.T. Toikka, J. Tuominiemi, E. Veikkola

Lappeenranta-Lahti University of Technology, Lappeenranta, Finland
N. Bin Norjoharuddeen, H. Kirschenmann, P. Luukka, H. Petrow

IRFU, CEA, Université Paris-Saclay, Gif-sur-Yvette, France
M. Besancon, F. Couderc, M. Dejardin, D. Denegri, P. Devouge, J.L. Faure, F. Ferri, P. Gaigne, S. Ganjour, P. Gras, F. Guilloux, G. Hamel de Monchenault, M. Kumar, V. Lohezic, Y. Maidannyk, J. Malcles, F. Orlandi, L. Portales, S. Ronchi, M.Ö. Sahin, P. Simkina, M. Titov, M. Tornago

Laboratoire Leprince-Ringuet, CNRS/IN2P3, Ecole Polytechnique, Institut Polytechnique de Paris, Palaiseau, France
R. Amella Ranz, F. Beaudette, K. Biriukov, G. Boldrini, P. Busson, C. Charlot, M. Chiusi, T.D. Cuisset, O. Davignon, A. De Wit, T. Debnath, I.T. Ehle,

S. Ghosh, A. Gilbert, R. Granier de Cassagnac, M. Manoni, M. Nguyen, S. Obraztsov, C. Ochando, L.m. Rabour, R. Salerno, J.B. Sauvan, Y. Sirois, G. Sokmen, Y. Song, L. Urda Gómez, B. Voirin, A. Zabi, A. Zghiche

Université de Strasbourg, CNRS, IPHC UMR 7178, Strasbourg, France
J.-L. Agram[19], J. Andrea, D. Bloch, E.C. Chabert, C. Collard, G. Coulon, C. Eschenlauer, S. Falke, U. Goerlach, A.-C. Le Bihan, G. Saha, A. Savoy-Navarro[20], P. Vaucelle

Centre de Calcul de l'Institut National de Physique Nucleaire et de Physique des Particules, CNRS/IN2P3, Villeurbanne, France
A. Di Florio, G. Mauceri, B. Orzari

Institut de Physique des 2 Infinis de Lyon (IP2I), Villeurbanne, France
D. Amram, S. Beauceron, B. Blancon, G. Boudoul, N. Chanon, D. Contardo, J. Daniel, P. Depasse, H. El Mamouni, J. Fay, E. Fillaudeau, S. Gascon, M. Gouzevitch, C. Greenberg, B. Ille, E. Jourd'Huy, M. Lethuillier, K. Long, B. Massoteau, L. Mirabito, A. Purohit, M. Vander Donckt, C. Verollet

Georgian Technical University, Tbilisi, Georgia
D. Chokheli, I. Lomidze, Z. Tsamalaidze[21]

RWTH Aachen University, I. Physikalisches Institut, Aachen, Germany
K.F. Adamowicz, V. Botta, S. Consuegra Rodríguez, L. Feld, K. Klein, M. Lipinski, P. Nattland, V. Oppenländer, A. Pauls, D. Pérez Adán

RWTH Aachen University, III. Physikalisches Institut A, Aachen, Germany
C. Daumann, S. Diekmann, E. Ehlert, N. Eich, D. Eliseev, F. Engelke, J. Erdmann, M. Erdmann, M.Z. Farkas, B. Fischer, T. Hebbeker, K. Hoepfner, A. Jung, N. Kumar, M.y. Lee, F. Mausolf, M. Merschmeyer, A. Meyer, A. Pozdnyakov, W. Redjeb, H. Reithler, U. Sarkar, V. Sarkisovi, A. Schmidt, J.G. Schulz, C. Seth, A. Sharma, J.L. Spah, V. Vaulin, U. Willemsen, S. Zaleski, F.P. Zinn

RWTH Aachen University, III. Physikalisches Institut B, Aachen, Germany
M.R. Beckers, G. Flügge, N. Hoeflich, T. Kress, A. Nowack, O. Pooth, A. Stahl

Deutsches Elektronen-Synchrotron, Hamburg, Germany
A. Abel, M. Aldaya Martin, J. Alimena, Y. An, I. Andreev, J. Bach, S. Baxter, H. Becerril Gonzalez, O. Behnke, F. Blekman[22], K. Borras[23], A. Campbell, S. Chatterjee, L.X. Coll Saravia, G. Eckerlin, D. Eckstein, E. Gallo[22], A. Geiser, M. Guthoff, A. Hinzmann, U. Husemann, M. Kasemann, C. Kleinwort, R. Kogler, M. Komm, D. Krücker, F. Labe, W. Lange, D. Leyva Pernia, J.h. Li, K.-Y. Lin, K. Lipka[24], W. Lohmann[25], J. Malvaso, R. Mankel, I.-A. Melzer-Pellmann, M. Mendizabal Morentin, A.B. Meyer, G. Milella, K. Moral Figueroa, A. Mussgiller, L.P. Nair, J. Niedziela, A. Nürnberg, J. Park, E. Ranken, A. Raspereza, D. Rastorguev, L. Rygaard, M. Scham[26,23], S. Schnake[23], P. Schütze, C. Schwanenberger[22], D. Schwarz, D. Selivanova, K. Sharko, M. Shchedrolosiev, A. Sritharan, D. Stafford, M. Torkian, S. Vashishtha, A. Ventura Barroso, R. Walsh, D. Wang, Q. Wang, K. Wichmann, L. Wiens[23], C. Wissing, Y. Yang, S. Zakharov, A. Zimermmane Castro Santos

University of Hamburg, Hamburg, Germany
A.R. Alves Andrade, M. Antonello, S. Bollweg, M. Bonanomi, L. Ebeling, K. El Morabit, Y. Fischer, M. Frahm, P.P. Gadow, E. Garutti, A. Grohsjean, A.A. Guvenli,

J. Haller, D. Hundhausen, M. Jalalvandi, G. Kasieczka, P. Keicher, R. Klanner, W. Korcari, T. Kramer, C.c. Kuo, J. Lange, B. Letzer, A. Lobanov, L. Markus, J. Matthiesen, L. Moureaux, K. Nikolopoulos, K.J. Pena Rodriguez, N. Prouvost, B. Raciti, M. Rieger, D. Savoiu, P. Schleper, M. Schröder, J. Schwandt, T. Tore von Schwartz, M. Sommerhalder, H. Stadie, G. Steinbrück, R. Ward, B. Wiederspan, M. Wolf, C. Yede

Karlsruher Institut fuer Technologie, Karlsruhe, Germany
A. Brusamolino, E. Butz, Y.M. Chen, T. Chwalek, A. Dierlamm, G.G. Dincer, U. Elicabuk, N. Faltermann, M. Giffels, A. Gottmann, F. Hartmann[27], F. Hummer, J. Kieseler, M. Klute, J. Knolle, H.A. Krause, R. Kunnilan Muhammed Rafeek, O. Lavoryk, J.M. Lawhorn, S. Maier, N. Meenamthuruthil Radhakrishnan, T. Mehner, M. Molch, A.A. Monsch, M. Mormile, Th. Müller, E. Pfeffer, M. Presilla, G. Quast, K. Rabbertz, B. Regnery, R. Schmieder, T. Selezneva, N. Shadskiy, I. Shvetsov, L. Sowa, L. Stockmeier, K. Tauqeer, M. Toms, B. Topko, N. Trevisani, C. Verstege, T. Voigtländer, R.F. Von Cube, J. Von Den Driesch, C. Winter, R. Wolf, W.D. Zeuner, X. Zuo

Institute of Nuclear and Particle Physics (INPP), NCSR Demokritos, Aghia Paraskevi, Greece
G. Anagnostou, G. Daskalakis, A. Kyriakis

National and Kapodistrian University of Athens, Athens, Greece
P. Iosifidou, P. Katris, M. Kotsarini, G. Melachroinos, Z. Painesis, N. Plastiras, N. Saoulidou, K. Theofilatos, E. Tzovara, K. Vellidis, I. Zisopoulos

National Technical University of Athens, Athens, Greece
T. Chatzistavrou, G. Karapostoli, K. Kousouris, K. Paschos, L.P. Rouseliotaki, E. Siamarkou, A. Taxeidi, G. Tsipolitis

University of Ioánnina, Ioánnina, Greece
I. Evangelou, C. Foudas, P. Katsoulis, P. Kokkas, P.G. Kosmoglou Kioseoglou, N. Manthos, I. Papadopoulos, J. Strologas

Democritus University of Thrace (DUTH), Kavala, Greece
E. Tziaferi

HUN-REN Wigner Research Centre for Physics, Budapest, Hungary
C. Hajdu, D. Horvath[28,29], Á. Kadlecsik, C. Lee, K. Márton, A.J. Rádl[30], F. Sikler, V. Veszpremi

MTA-ELTE Lendület CMS Particle and Nuclear Physics Group, Eötvös Loránd University, Budapest, Hungary
G. Balint, M. Csanád, K. Farkas, A. Fehérkuti[31], M.M.A. Gadallah[32], M. León Coello, G. Pásztor, G.I. Veres

Faculty of Informatics, University of Debrecen, Debrecen, Hungary
D. Baranyai, B. Ujvari

HUN-REN ATOMKI - Institute of Nuclear Research, Debrecen, Hungary
G. Bencze, S. Czellar, J. Molnar, Z. Szillasi

Karoly Robert Campus, MATE Institute of Technology, Gyongyos, Hungary
T. Csorgo[31], F. Nemes[31], T. Novak, I. Szanyi[33]

IIT Bhubaneswar, Bhubaneswar, India
S. Bahinipati, R. Raturi

Panjab University, Chandigarh, India
S. Bansal, V. Bhatnagar, B. Chauhan, S. Chauhan, N. Dhingra[34], A. Kaur, H. Kaur, S. Kumar, T. Sheokand, A. Singla, K. Verma

University of Delhi, Delhi, India
A. Bhardwaj, A. Chhetri, B.C. Choudhary, A. Kumar, A. Kumar, M. Naimuddin, S. Phor, C. Prakash, K. Ranjan, M.K. Saini

Indian Institute of Technology Mandi (IIT-Mandi), Himachal Pradesh, India
M. Kumari, P. Palni, S. Rana, A. Rathore, A. Sarkar

University of Hyderabad, Hyderabad, India
S. Acharya[35], B. Gomber, S.K. Satapathy

Indian Institute of Technology Kanpur, Kanpur, India
S. Mukherjee

Saha Institute of Nuclear Physics, HBNI, Kolkata, India
S. Bhattacharya, S. Das Gupta, S. Dutta, S. Dutta, S. Sarkar

Indian Institute of Technology Madras, Madras, India
M.M. Ameen, P.K. Behera, S. Chatterjee, G. Dash, A. Dattamunsi, P. Jana, P. Kalbhor, S. Kamble, J.R. Komaragiri[36], P.R. Pujahari, A.K. Sikdar, R.K. Singh, P. Verma, S. Verma, A. Vijay

IISER Mohali, India, Mohali, India
A. Chauhan, S. Nayak, H. Rajpoot, B.K. Sirasva

Tata Institute of Fundamental Research-A, Mumbai, India
L. Bhatt, S. Dugad, T. Mishra, G.B. Mohanty, M. Shelake, P. Suryadevara

Tata Institute of Fundamental Research-B, Mumbai, India
A. Bala, S. Banerjee, S. Barman[37], R.M. Chatterjee, J. Chhikara, M. Guchait, Sh. Jain, A. Jaiswal, S. Kumar, M. Maity[37], G. Majumder, K. Mazumdar, R. Pramanik, R. Saxena, P. Sharma, A. Thachayath

National Institute of Science Education and Research, An OCC of Homi Bhabha National Institute, Bhubaneswar, Odisha, India
R. Kumar Agrawal, D. Maity[38], P. Mal, K. Naskar[38], A. Nayak[38], K. Pal, P. Sadangi, S. Shuchi, S.K. Swain, S. Varghese[38], D. Vats[38]

Indian Institute of Science Education and Research (IISER), Pune, India
S. Dube, P. Hazarika, B. Kansal, A. Laha, R. Sharma, S. Sharma, K.Y. Vaish

Indian Institute of Technology Hyderabad, Telangana, India
C. Agrawal, B. Babu, S. Ghosh

Isfahan University of Technology, Isfahan, Iran
H. Bakhshiansohi[39], A. Jafari[40], V. Sedighzadeh Dalavi, M. Zeinali[41]

Institute for Research in Fundamental Sciences (IPM), Tehran, Iran
S. Bashiri, S. Chenarani[42], S.M. Etesami, Y. Hosseini, M. Khakzad, E. Khazaie, M. Mohammadi Najafabadi, M. Nourbakhsh, S. Tizchang[43]

University College Dublin, Dublin, Ireland
M. Felcini, M. Grunewald

INFN Sezione di Bari[a], Università di Bari[b], Politecnico di Bari[c], Bari, Italy
M. Abbrescia[a,b], M. Buonsante[a,b], A. Colaleo[a,b], D. Creanza[a,c], N. De Filippis[a,c], M. De Palma[a,b], W. Elmetenawee[a,b,16], N. Ferrara[a,c], L. Fiore[a], L. Generoso[a,b], L. Longo[a], M. Louka[a,b], G. Maggi[a,c], M. Maggi[a], S. My[a,b], F. Nenna[a,b], A. Pellecchia[a,b], A. Pompili[a,b], F.M. Procacci[a,b], G. Pugliese[a,c], R. Radogna[a,b], D. Ramos[a], A. Ranieri[a], L. Silvestris[a], F.M. Simone[a,b], Ü. Sözbilir[a,44], A. Stamerra[a,b], D. Troiano[a,b], R. Venditti[a,b], P. Verwilligen[a], A. Zaza[a,b]

INFN Sezione di Bologna[a], Università di Bologna[b], Bologna, Italy
G. Abbiendi[a], S. Balducci[a,b], C. Battilana[a,b], D. Bonacorsi[a,b], P. Capiluppi[a,b], F.R. Cavallo[a], M. Cruciani[a,b], G.M. Dallavalle[a], T. Diotalevi[a,b], F. Fabbri[a], A. Fanfani[a,b], R. Farinelli[a], D. Fasanella[a], L. Ferragina[a,b], P. Giacomelli[a], C. Grandi[a], L. Guiducci[a,b], M. Lorusso[a,b], L. Lunerti[a], S. Marcellini[a], G. Masetti[a], F.L. Navarria[a,b], G. Paggi[a,b], A. Perrotta[a], A.M. Rossi[a,b], S. Rossi Tisbeni[a,b], G.P. Siroli[a,b]

INFN Sezione di Catania[a], Università di Catania[b], Catania, Italy
S. Costa[a,b,45], A. Di Mattia[a], A. Lapertosa[a], R. Potenza[a,b], A. Tricomi[a,b,45]

INFN Sezione di Firenze[a], Università di Firenze[b], Firenze, Italy
J. Altork[a,b], G. Barbagli[a], G. Bardelli[a], A. Calandri[a,b], B. Camaiani[a,b], A. Cassese[a], R. Ceccarelli[a], V. Ciulli[a,b], C. Civinini[a], R. D'Alessandro[a,b], L. Damenti[a,b], E. Focardi[a,b], T. Kello[a], G. Latino[a,b], P. Lenzi[a,b], M. Lizzo[a], M. Meschini[a], S. Paoletti[a], A. Papanastassiou[a,b], G. Sguazzoni[a], L. Viliani[a]

INFN Laboratori Nazionali di Frascati, Frascati, Italy
L. Benussi, S. Colafranceschi[46], S. Meola[47], D. Piccolo

INFN Sezione di Genova[a], Università di Genova[b], Genova, Italy
M. Alves Gallo Pereira[a], F. Ferro[a], E. Robutti[a], S. Tosi[a,b]

INFN Sezione di Milano-Bicocca[a], Università di Milano-Bicocca[b], Milano, Italy
A. Benaglia[a], F. Brivio[a], V. Camagni[a,b], F. Cetorelli[a,b], F. De Guio[a,b], M.E. Dinardo[a,b], P. Dini[a], S. Gennai[a], R. Gerosa[a,b], A. Ghezzi[a,b], P. Govoni[a,b], L. Guzzi[a], G. Lavizzari[a,b], M.T. Lucchini[a,b], M. Malberti[a], S. Malvezzi[a], A. Massironi[a], L. Moroni[a], M. Paganoni[a,b], S. Palluotto[a,b], D. Pedrini[a], A. Perego[a,b], T. Tabarelli de Fatis[a,b]

INFN Sezione di Napoli[a], Università di Napoli 'Federico II'[b], Napoli, Italy; Università della Basilicata[c], Potenza, Italy; Scuola Superiore Meridionale (SSM)[d], Napoli, Italy
S. Buontempo[a], F. Confortini[a,b], C. Di Fraia[a,b], F. Fabozzi[a,c], L. Favilla[a,d], A.O.M. Iorio[a,b], L. Lista[a,b,48], P. Paolucci[a,27], B. Rossi[a]

INFN Sezione di Padova[a], Università di Padova[b], Padova, Italy; Universita degli Studi di Cagliari[c], Cagliari, Italy
P. Azzi[a], N. Bacchetta[a,49], D. Bisello[a,b], L. Borella[a], P. Bortignon[a,c], G. Bortolato[a,b], A.C.M. Bulla[a,c], R. Carlin[a,b], P. Checchia[a], T. Dorigo[a,50], F. Gasparini[a,b], U. Gasparini[a,b], S. Giorgetti[a], P. Grutta[a], N. Lai[a], E. Lusiani[a], M. Margoni[a,b], A.T. Meneguzzo[a,b], M. Missiroli[a], J. Pazzini[a,b], F. Primavera[a,b], P. Ronchese[a,b], R. Rossin[a,b], F. Simonetto[a,b], M. Toffano[a], M. Tosi[a,b], A. Triossi[a,b], S. Ventura[a], M. Zanetti[a,b], P. Zotto[a,b], A. Zucchetta[a,b], G. Zumerle[a,b]

INFN Sezione di Pavia[a], Università di Pavia[b], Pavia, Italy
S. Abu Zeid[a,51], C. Aimè[a], A. Braghieri[a], M. Brunoldi[a,b], P. Montagna[a,b], M. Pelliccioni[a,b], V. Re[a], C. Riccardi[a,b], P. Salvini[a], I. Vai[a,b], P. Vitulo[a,b]

INFN Sezione di Perugia[a], Università di Perugia[b], Perugia, Italy
S. Ajmal[a,b], M.E. Ascioti[a,b], G.M. Bilei[†a], W.D. Buitrago Ceballos[a,b], C. Carrivale[a,b], D. Ciangottini[a,b], L. Della Penna[a,b], L. Fanò[a,b], V. Mariani[a,b], M. Menichelli[a], F. Moscatelli[a,52], A. Rossi[a,b], A. Santocchia[a,b], D. Spiga[a], T. Tedeschi[a,b]

INFN Sezione di Pisa[a], Università di Pisa[b], Scuola Normale Superiore di Pisa[c], Pisa, Italy; Università di Siena[d], Siena, Italy
C.A. Alexe[a,c], P. Asenov[a,b], P. Azzurri[a], G. Bagliesi[a], L. Bianchini[a,b], T. Boccali[a], E. Bossini[a], D. Bruschini[a,c], R. Castaldi[a], F. Cattafesta[a,c], M.A. Ciocci[a,d], M. Cipriani[a,b], R. Dell'Orso[a], S. Dhani[a,d], S. Donato[a,b], A. Feliziani[a,d], R. Forti[a,b], A. Giassi[a], F. Ligabue[a,c], A.C. Marini[a,b], A. Messineo[a,b], S. Mishra[a], V.K. Muraleedharan Nair Bindhu[a,b], S. Nandan[a], F. Palla[a], M. Riggirello[a,c], A. Rizzi[a,b], G. Rolandi[a,c], A. Scribano[a], P. Solanki[a,b], P. Spagnolo[a], F. Tenchini[a,b], R. Tenchini[a], G. Tonelli[a,b], N. Turini[a,d], F. Vaselli[a,c], A. Venturi[a], P.G. Verdini[a]

INFN Sezione di Roma[a], Sapienza Università di Roma[b], Roma, Italy
P. Akrap[a,b], C. Basile[a,b], S.C. Behera[a], F. Cavallari[a], L. Cunqueiro Mendez[a,b], F. De Riggi[a,b], D. Del Re[a,b], M. Del Vecchio[a,b], E. Di Marco[a], M. Diemoz[a], F. Errico[a], L. Frosina[a,b], R. Gargiulo[a,b], B. Harikrishnan[a,b], F. Lombardi[a,b], L. Martikainen[a,b], G. Organtini[a,b], N. Palmeri[a,b], R. Paramatti[a,b], T. Pauletto[a,b], S. Rahatlou[a,b], C. Rovelli[a], F. Santanastasio[a,b], L. Soffi[a], V. Vladimirov[a,b]

INFN Sezione di Torino[a], Università di Torino[b], Torino, Italy; Università del Piemonte Orientale[c], Novara, Italy
N. Amapane[a,b], R. Arcidiacono[a,c], S. Argiro[a,b], M. Arneodo[†a,c], N. Bartosik[a,c], F. Bashir[a,b], R. Bellan[a,b], A. Bellora[a,b], C. Biino[a], C. Borca[a,b], N. Cartiglia[a], M. Costa[a,b], R. Covarelli[a,b], N. Demaria[a], E. Ferrando[a,b], L. Finco[a], M. Grippo[a,b], B. Kiani[a,b], L. Lanteri[a,b], F. Luongo[a,b], M. Marchisio Caprioglio[a,b], C. Mariotti[a], S. Maselli[a], A. Mecca[a,b], L. Menzio[a,b], P. Meridiani[a], E. Migliore[a,b], M. Monteno[a], M.M. Obertino[a,b], G. Ortona[a], L. Pacher[a,b], N. Pastrone[a], M. Ruspa[a,c], F. Siviero[a,b], V. Sola[a,b], A. Solano[a,b], A. Staiano[a], C. Tarricone[a,b], D. Trocino[a], G. Umoret[a,b], E. Vlasov[a,b], R. White[a,b]

INFN Sezione di Trieste[a], Università di Trieste[b], Trieste, Italy
J. Babbar[a,b,53], S. Belforte[a], V. Candelise[a,b], M. Casarsa[a], F. Cossutti[a], K. De Leo[a], G. Della Ricca[a,b], R. Delli Gatti[a,b], C. Giraldin[a,b]

Kyungpook National University, Daegu, Korea
S. Dogra, J. Hong, J. Kim, J. Kim, T. Kim, D. Lee, H. Lee, J. Lee, S.W. Lee, C.S. Moon, Y.D. Oh, S. Sekmen, B. Tae, Y.C. Yang

Department of Mathematics and Physics - GWNU, Gangneung, Korea
M.S. Kim

Chonnam National University, Institute for Universe and Elementary Particles, Kwangju, Korea
G. Bak, P. Gwak, H. Kim, H. Lee, S. Lee, D.H. Moon, J. Seo

Department of Physics, Chung-Ang University, Seoul, Korea

K. Lee, Y. Lee

Hanyang University, Seoul, Korea
E. Asilar, F. Carnevali, J. Choi[54], T.J. Kim, Y. Ryou, J. Song, T. Yang

Korea University, Seoul, Korea
S. Ha, B. Hong, J. Kim, K. Lee, K. Lee, S. Lee, J. Padmanaban, B.A.N. Putra, J. Yoo

Kyung Hee University, Department of Physics, Seoul, Korea
J. Goh, J. Shin, S. Yang

Sejong University, Seoul, Korea
L. Kalipoliti, Y. Kang, H. S. Kim, Y. Kim, B. Ko, S. Lee

Seoul National University, Seoul, Korea
J.H. Bhyun, J. Choi, J. Choi, W. Jun, H. Kim, J. Kim, J. Kim, T. Kim, Y. Kim, Y.W. Kim, S. Ko, H. Lee, J. Lee, J. Lee, B.H. Oh, J. Shin, U.K. Yang, I. Yoon

University of Seoul, Seoul, Korea
S. Calzaferri, W. Heo, W. Jang, D. Kim, S. Kim, J.S.H. Lee, Y. Roh, I.J. Watson

Yonsei University, Department of Physics, Seoul, Korea
G. Cho, Y. Eo, K. Hwang, H. Jang, B. Kim, D. Kim, S. Kim, G. Mocellin, H.D. Yoo

Sungkyunkwan University, Suwon, Korea
Y. Lee, I. Yu

College of Engineering and Technology, American University of the Middle East (AUM), Dasman, Kuwait
T. Beyrouthy, Y. Gharbia

Kuwait University - College of Science - Department of Physics, Safat, Kuwait
F. Alazemi

Riga Technical University, Riga, Latvia
K. Dreimanis, O.M. Eberlins, A. Gaile, J.K. Heikkilä, M. Klevs, C. Munoz Diaz, D. Osite, G. Pikurs, R. Plese, A. Potrebko, M. Seidel, D. Sidiropoulos Kontos

University of Latvia (LU), Riga, Latvia
N.R. Strautnieks

Vilnius University, Vilnius, Lithuania
M. Ambrozas, A. Juodagalvis, S. Nargelas, S. Nayak, G. Tamulaitis

National Centre for Particle Physics, Universiti Malaya, Kuala Lumpur, Malaysia
I. Yusuff[55], Z. Zolkapli

Universidad de Sonora (UNISON), Hermosillo, Mexico
J.P. Barajas Ibarria, J.F. Benitez, A. Castaneda Hernandez, A. Cota Rodriguez, L.E. Cuevas Picos, H.A. Encinas Acosta, L.G. Gallegos Maríñez, J.A. Murillo Quijada, L. Valencia Palomo

Centro de Investigacion y de Estudios Avanzados del IPN, Mexico City, Mexico
G. Ayala, H. Castilla-Valdez, H. Crotte Ledesma, R. Lopez-Fernandez, J. Mejia Guisao, R. Reyes-Almanza, A. Sánchez Hernández

Universidad Iberoamericana, Mexico City, Mexico
C. Oropeza Barrera, D.L. Ramirez Guadarrama, M. Ramírez García

Benemerita Universidad Autonoma de Puebla, Puebla, Mexico
I. Bautista, F.E. Neri Huerta, I. Pedraza, H.A. Salazar Ibarguen, C. Uribe Estrada

University of Montenegro, Podgorica, Montenegro
I. Bubanja, J. Mijuskovic, N. Raicevic

National Centre for Physics, Quaid-I-Azam University, Islamabad, Pakistan
A. Ahmad, M.I. Asghar, A. Awais, M.I.M. Awan, W.A. Khan, I. Sohail

AGH University of Krakow, Krakow, Poland
V. Avati, L. Forthomme, L. Grzanka, M. Malawski, K. Piotrzkowski

National Centre for Nuclear Research, Swierk, Poland
H. Awedikian, M. Bluj, M. Ghimiray, M. Górski, M. Kazana, M. Szleper, P. Zalewski

Institute of Experimental Physics, Faculty of Physics, University of Warsaw, Warsaw, Poland
K. Bunkowski, K. Doroba, A. Kalinowski, M. Konecki, J. Krolikowski, W. Matyszkiewicz, A. Muhammad, S. Slawinski

Warsaw University of Technology, Warsaw, Poland
P. Fokow, K. Pozniak, W. Zabolotny

Laboratório de Instrumentação e Física Experimental de Partículas, Lisboa, Portugal
M. Araujo, C. Beirão Da Cruz E Silva, A. Boletti, M. Bozzo, T. Camporesi[56,57], G. Da Molin, M. Gallinaro, R. Guitton, J. Hollar, H. Legoinha, N. Leonardo[58], G.B. Marozzo, A. Petrilli, M. Pisano, J. Seixas, J. Varela, J.W. Wulff

Faculty of Physics, University of Belgrade, Belgrade, Serbia
P. Adzic, L. Markovic, P. Milenovic, V. Milosevic

VINCA Institute of Nuclear Sciences, University of Belgrade, Belgrade, Serbia
D. Devetak, M. Dordevic, J. Milosevic, L. Nadderd, V. Rekovic, M. Stojanovic

Centro de Investigaciones Energéticas Medioambientales y Tecnológicas (CIEMAT), Madrid, Spain
M. Alcalde Martinez, J. Alcaraz Maestre, Cristina F. Bedoya, J.A. Brochero Cifuentes, Oliver M. Carretero, M. Cepeda, M. Cerrada, N. Colino, B. De La Cruz, A. Escalante Del Valle, D. Fernández Del Val, J.P. Fernández Ramos, J. Flix, M.C. Fouz, M. Gonzalez Hernandez, O. Gonzalez Lopez, S. Goy Lopez, J.M. Hernandez, M.I. Josa, J. Llorente Merino, C. Martin Perez, E. Martin Viscasillas, D. Moran, C. M. Morcillo Perez, Á. Navarro Tobar, A. Pérez-Calero Yzquierdo, J. Puerta Pelayo, I. Redondo, D.D. Redondo Ferrero, J. Vazquez Escobar

Universidad Autónoma de Madrid, Madrid, Spain
J.F. de Trocóniz

Universidad de Oviedo, Instituto Universitario de Ciencias y Tecnologías Espaciales de Asturias (ICTEA), Oviedo, Spain
E. Aller Gutierrez, B. Alvarez Gonzalez, J. Ayllon Torresano, A. Cardini, J. Cuevas, J. Del Riego Badas, D. Estrada Acevedo, J. Fernandez Menendez, S. Folgueras, I. Gonzalez Caballero, P. Leguina, M. Obeso Menendez, E. Palencia Cortezon, J. Prado Pico, S. Sanchez Cruz, A. Soto Rodríguez, P. Vischia

Instituto de Física de Cantabria (IFCA), CSIC-Universidad de Cantabria, Santander, Spain
S. Blanco Fernández, I.J. Cabrillo, A. Calderon, M. Caserta, J. Duarte Campderros,

M. Fernandez, G. Gomez, C. Lasaosa García, R. Lopez Ruiz, C. Martinez Rivero, P. Martinez Ruiz del Arbol, F. Matorras, P. Matorras Cuevas, E. Navarrete Ramos, J. Piedra Gomez, C. Quintana San Emeterio, V. Rodriguez, L. Scodellaro, I. Vila, R. Vilar Cortabitarte, J.M. Vizan Garcia

University of Colombo, Colombo, Sri Lanka
B. Kailasapathy[59]

University of Ruhuna, Department of Physics, Matara, Sri Lanka
W.G.D. Dharmaratna[60], N. Perera

CERN, European Organization for Nuclear Research, Geneva, Switzerland
D. Abbaneo, C. Amendola, R. Ardino, E. Auffray, J. Baechler, D. Barney, J. Bendavid, I. Bestintzanos, M. Bianco, A. Bocci, L. Borgonovi, C. Botta, A. Bragagnolo, C.E. Brown, C. Caillol, G. Cerminara, P. Connor, K. Cormier, D. d'Enterria, A. Dabrowski, P. Das, A. David, A. De Roeck, M.M. Defranchis, M. Deile, M. Dobson, P.J. Fernández Manteca, E. Fialova, B.A. Fontana Santos Alves, E. Fontanesi, W. Funk, A. Gaddi, S. Giani, D. Gigi, K. Gill, F. Glege, M. Glowacki, A. Gruber, J. Hegeman, R. Hofsaess, B. Huber, T. James, P. Janot, L. Jeppe, O. Kaluzinska, O. Karacheban[25], G. Karathanasis, S. Laurila, P. Lecoq, J. León Holgado, E. Leutgeb, C. Lourenço, A.-M. Lyon, M. Magherini, L. Malgeri, E. Manca, M. Mannelli, F. Meijers, J.A. Merlin, S. Mersi, E. Meschi, M. Migliorini, F. Monti, F. Moortgat, M.C. Muehlnikel, M. Mulders, M. Musich, I. Neutelings, S. Orfanelli, F. Pantaleo, M. Pari, F. Pereira Carneiro, G. Petrucciani, A. Pfeiffer, M. Pierini, M. Pitt, H. Qu, A. Reimers, B. Ribeiro Lopes, F. Riti, P. Rosado, M. Rovere, H. Sakulin, R. Salvatico, S. Scarfi, S.F. Schaefer, M. Selvaggi, P. Silva, P. Sphicas[61], A.G. Stahl Leiton, A. Steen, S. Summers, G. Terragni, D. Treille, P. Tropea, E. Vernazza, M. Vojinovic, J. Wanczyk[62], S. Wuchterl, M. Zarucki, P. Zehetner, P. Zejdl, G. Zevi Della Porta

PSI Center for Neutron and Muon Sciences, Villigen, Switzerland
L. Caminada[63], W. Erdmann, R. Horisberger, Q. Ingram, H.C. Kaestli, D. Kotlinski, C. Lange, U. Langenegger, A. Nigamova, L. Noehte[63], L. Redard-Jacot[63], T. Rohe, A. Samalan

ETH Zurich - Institute for Particle Physics and Astrophysics (IPA), Zurich, Switzerland
T.K. Aarrestad, M. Backhaus, A. Belvedere, T. Bevilacqua[63], G. Bonomelli, C. Cazzaniga, K. Datta, P. De Bryas Dexmiers D'Archiacchiac[62], A. De Cosa, G. Dissertori, M. Dittmar, M. Donegà, F. Glessgen, C. Grab, N. Härringer, T.G. Harte, B. Kaynak, M.Köppel, W. Lustermann, M. Malucchi, R.A. Manzoni, L. Marchese, F. Nessi-Tedaldi, F. Pauss, A.A. Petre, J. Prendi, B. Ristic, S. Rohletter, P.M. Sander, R. Seidita, J. Steggemann[62], A. Tarabini, C.Z. Tee, D. Valsecchi, P.H. Wagner, R. Wallny

Universität Zürich, Zurich, Switzerland
C. Amsler[64], P. Bärtschi, F. Bilandzija, M.F. Canelli, G. Celotto, Z. Ghafoor, T.A. Goldschmidt, V. Guglielmi, A. Jofrehei, B. Kilminster, T.H. Kwok, S. Leontsinis, V. Lukashenko, A. Macchiolo, F. Meng, J. Motta, P. Robmann, E. Shokr, F. Stäger, R. Tramontano, P. Viscone

National Central University, Chung-Li, Taiwan
D. Bhowmik, Y.h. Chou, C.M. Kuo, P.K. Rout, S. Taj, P.C. Tiwari[36]

National Taiwan University (NTU), Taipei, Taiwan
L. Ceard, K.F. Chen, Z.g. Chen, A. De Iorio, W.-S. Hou, T.h. Hsu, Y.w. Kao, S. Karmakar, F. Khuzaimah, G. Kole, Y.y. Li, R.-S. Lu, E. Paganis, X.f. Su, J. Thomas-Wilsker, L.s. Tsai, D. Tsionou, H.y. Wu, E. Yazgan

High Energy Physics Research Unit, Department of Physics, Faculty of Science, Chulalongkorn University, Bangkok, Thailand
C. Asawatangtrakuldee, N. Srimanobhas

Tunis El Manar University, Tunis, Tunisia
Y. Maghrbi

Çukurova University, Physics Department, Science and Art Faculty, Adana, Turkey
D. Agyel, F. Dolek, I. Dumanoglu[65], Y. Guler[66], E. Gurpinar Guler[66], A. Kayis Topaksu, G. Onengut, K. Ozdemir[67], B. Tali[68], U.G. Tok, E. Uslan

Hacettepe University, Ankara, Turkey
S. Sen

Bogazici University, Istanbul, Turkey
B. Akgun, I.O. Atakisi[69], E. Gülmez, M. Kaya[70], O. Kaya[71], M.A. Sarkisla[72], S. Tekten[73]

Istanbul Technical University, Istanbul, Turkey
D. Boncukcu, A. Cakir, K. Cankocak[65,74], M. Gumustekin, A.D. Gungordu

Istanbul University, Istanbul, Turkey
B. Hacisahinoglu, I. Hos[75], S. Ozkorucuklu, O. Potok, H. Sert, C. Simsek, C. Zorbilmez

Yildiz Technical University, Istanbul, Turkey
S. Cerci, C. Dozen[76], E. Iren[77], B. Isildak, E. Simsek, D. Sunar Cerci, T. Yetkin[76]

Institute for Scintillation Materials of National Academy of Science of Ukraine, Kharkiv, Ukraine
O. Dadazhanova, B. Grynyov

National Science Centre, Kharkiv Institute of Physics and Technology, Kharkiv, Ukraine
K. Klimenko, O. Kurov, L. Levchuk, S. Lukyanenko, A. Pristavka, D. Soroka

University of Bristol, Bristol, United Kingdom
J.J. Brooke, A. Bundock, F. Bury, E. Clement, D. Cussans, D. Dharmender, H. Flacher, J. Goldstein, H.F. Heath, M.-L. Holmberg, A. Karakoulaki, L. Kreczko, S. Paramesvaran, L. Robertshaw, M.S. Sanjrani[39], J. Segal, V.J. Smith

Rutherford Appleton Laboratory, Didcot, United Kingdom
A.H. Ball, K.W. Bell, A. Belyaev[78], C. Brew, R.M. Brown, D.J.A. Cockerill, A. Elliot, K.V. Ellis, J. Gajownik, K. Harder, S. Harper, J. Linacre, K. Manolopoulos, M. Moallemi, D.M. Newbold, E. Olaiya, D. Petyt, T. Reis, A.R. Sahasransu, T. Schuh, C.H. Shepherd-Themistocleous, I.R. Tomalin, K.C. Whalen, T. Williams

Imperial College, London, United Kingdom
I. Andreou, S. Awan, R. Bainbridge, P. Bloch, O. Buchmuller, C.A. Carrillo Montoya, D. Colling, A. Cox, I. Das, P. Dauncey, G. Davies, M. Della Negra, S. Fayer, G. Fedi, G. Hall, H.R. Hoorani, A. Howard, G. Iles, C.R. Knight, P. Krueper, J. Langford, K.H. Law, L. Lyons, A.-M. Magnan, B. Maier, S. Mallios,

A. Mastronikolis, J. Nash[79], M. Pesaresi, P.B. Pradeep, E.V. Protopapa, B.C. Radburn-Smith, A. Richards, A. Rose, T.B. Runting, L. Russell, K. Savva, R. Schmitz, C. Seez, R. Shukla, A. Tapper, T. Travis, K. Uchida, G.P. Uttley, T. Virdee[27], N. Wardle, D. Winterbottom, J. Xiao

Brunel University, Uxbridge, United Kingdom
J.E. Cole, L. Juckett, A. Khan, P. Kyberd, I.D. Reid

Baylor University, Waco, Texas, USA
S. Abdullin, A. Brinkerhoff, E. Collins, M.R. Darwish, J. Dittmann, K. Hatakeyama, V. Hegde, J. Hiltbrand, B. McMaster, J. Samudio, S. Sawant, C. Sutantawibul, J. Wilson

Bethel University, St. Paul, Minnesota, USA
J.M. Hogan

Catholic University of America, Washington, DC, USA
R. Bartek, A. Dominguez, S. Raj, B. Sahu, A.E. Simsek, B. Singhal, S.S. Yu

The University of Alabama, Tuscaloosa, Alabama, USA
B. Bam, A. Buchot Perraguin, S. Campbell, R. Chudasama, S.I. Cooper, C. Crovella, G. Fidalgo, S.V. Gleyzer, R. Kaur, A. Khukhunaishvili, K. Matchev, E. Pearson, P. Rumerio[80], E. Usai, R. Yi

Boston University, Boston, Massachusetts, USA
S. Cholak, Z. Demiragli, C. Erice, C. Fangmeier, C. Fernandez Madrazo, J. Fulcher, J. Garcia De Castro, F. Golf, S. Jeon, G. Linney, J. O'Cain, I. Reed, J. Rohlf, D. Sperka, I. Suarez, A. Tsatsos, E. Wurtz, A.G. Zecchinelli

Brown University, Providence, Rhode Island, USA
G. Barone, G. Benelli, D. Cutts, S. Ellis, S. Gottlieb, L. Gouskos, M. Hadley, L. Hay, U. Heintz, K.W. Ho, R. Jain, T. Kwon, L. Lambrecht, G. Landsberg, K.T. Lau, M. LeBlanc, J. Luo, S. Mondal, J. Roloff, T. Russell, S. Sagir[81], X. Shen, M. Stamenkovic, S. Sunnarborg, J. Tang, N. Venkatasubramanian

University of California, Davis, Davis, California, USA
S. Abbott, S. Baradia, B. Barton, R. Breedon, H. Cai, M. Calderon De La Barca Sanchez, E. Cannaert, M. Chertok, M. Citron, J. Conway, P.T. Cox, F. Eble, R. Erbacher, C. Fairchild, O. Kukral, S. Ostrom, I. Salazar Segovia, J.H. Steenis, J.S. Tafoya Vargas, W. Wei, S. Yoo

University of California, Los Angeles, California, USA
K. Adamidis, H. Ancelin, M. Bachtis, D. Campos, R. Cousins, S. Crossley, G. Flores Avila, J. Hauser, M. Ignatenko, M.A. Iqbal, T. Lam, Y.f. Lo, A. Nunez Del Prado, D. Saltzberg, V. Valuev

University of California, Riverside, Riverside, California, USA
R. Clare, J.W. Gary, G. Hanson

University of California, San Diego, La Jolla, California, USA
A. Aportela, A. Arora, J.G. Branson, S. Cittolin, B. D'Anzi, D. Diaz, J. Duarte, L. Giannini, Y. Gu, J. Guiang, V. Krutelyov, R. Lee, J. Letts, H. Li, R. Marroquin Solares, M. Masciovecchio, F. Mokhtar, S. Morovic, S. Mukherjee, M. Pieri, D. Primosch, M. Quinnan, V. Sharma, M. Tadel, E. Vourliotis, F. Würthwein, A. Yagil, Z. Zhao

University of California, Santa Barbara - Department of Physics, Santa Barbara, California, USA
A. Barzdukas, L. Brennan, C. Campagnari, S. Carron Montero[82], K. Downham, C. Grieco, J.S. Guo, M.M. Hussain, D. Imani, J. Incandela, M.W.K. Lai, A.J. Li, P. Masterson, J.J.H. Ockenfuss, J. Richman, S.N. Santpur, D. Stuart, T.Á. Vámi, X. Yan, D. Zhang

California Institute of Technology, Pasadena, California, USA
A. Albert, S. Bhattacharya, A. Bornheim, O. Cerri, Z. Hao, L. Mori, H.B. Newman, T. Sievert, P. Simmerling, E. Sledge, M. Spiropulu, C. Sun, J.R. Vlimant, R.A. Wynne, S. Xie, R.Y. Zhu

Carnegie Mellon University, Pittsburgh, Pennsylvania, USA
J. Alison, S. An, M. Cremonesi, V. Dutta, E.Y. Ertorer, T. Ferguson, T.A. Gómez Espinosa, A. Harilal, A. Kallil Tharayil, M. Kanemura, A. Khanal, C. Liu, M. Marchegiani, P. Meiring, S. Murthy, P. Palit, K. Park, M. Paulini, A. Roberts, A. Sanchez, Y. Zhou

University of Colorado Boulder, Boulder, Colorado, USA
J.P. Cumalat, W.T. Ford, J. Fraticelli, A. Hart, M. Herrmann, S. Kwan, J. Pearkes, N. Schonbeck, K. Stenson, K.A. Ulmer, S.R. Wagner, N. Zipper, D. Zuolo

Cornell University, Ithaca, New York, USA
J. Alexander, X. Chen, G. De Castro, J. Dickinson, A. Duquette, J. Fan, X. Fan, J. Grassi, P. Kotamnives, K. Krzyzanska, J. Monroy, G. Niendorf, M. Oshiro, J.R. Patterson, A. Ryd, J. Thom, H.A. Weber, B. Weiss, P. Wittich, Y. Wu, R. Zou, L. Zygala

Fermi National Accelerator Laboratory, Batavia, Illinois, USA
M. Albrow, M. Alyari, O. Amram, G. Apollinari, A. Apresyan, L.A.T. Bauerdick, D. Berry, J. Berryhill, P.C. Bhat, K. Burkett, J.N. Butler, A. Canepa, G.B. Cerati, H.W.K. Cheung, F. Chlebana, C. Cosby, G. Cummings, I. Dutta, V.D. Elvira, J. Freeman, A. Gandrakota, Z. Gecse, L. Gray, D. Green, A. Grummer, S. Grünendahl, D. Guerrero, O. Gutsche, R.M. Harris, J. Hirschauer, V. Innocente, B. Jayatilaka, S. Jindariani, M. Johnson, R.S. Kim, S. Lammel, D. Lincoln, R. Lipton, T. Liu, K. Maeshima, D. Mason, P. McBride, P. Merkel, S. Mrenna, S. Nahn, J. Ngadiuba, D. Noonan, S. Norberg, V. Papadimitriou, N. Pastika, K. Pedro, C. Pena[83], C.E. Perez Lara, V. Perovic, F. Ravera, A. Reinsvold Hall[84], L. Ristori, M. Safdari, E. Sexton-Kennedy, E. Smith, N. Smith, A. Soha, L. Spiegel, S. Stoynev, J. Strait, L. Taylor, S. Tkaczyk, N.V. Tran, L. Uplegger, E.W. Vaandering, C. Wang, I. Zoi

University of Florida, Gainesville, Florida, USA
C. Aruta, P. Avery, D. Bourilkov, P. Chang, V. Cherepanov, M. Dittrich, R.D. Field, C. Huh, E. Koenig, M. Kolosova, J. Konigsberg, A. Korytov, G. Mitselmakher, K. Mohrman, A. Muthirakalayil Madhu, N. Rawal, S. Rosenzweig, Y. Takahashi, J. Wang

Florida State University, Tallahassee, Florida, USA
T. Adams, A. Al Kadhim, D. Alam, A. Askew, S. Bower, R. Goff, R. Hashmi, A. Hassani, T. Kolberg, G. Martinez, M. Mazza, H. Prosper, P.R. Prova, R. Yohay

Florida Institute of Technology, Melbourne, Florida, USA

B. Alsufyani, S. Das, S. Demarest, L. Hasa, M. Hohlmann, M. Lavinsky, E. Yanes

University of Illinois Chicago, Chicago, Illinois, USA
M.R. Adams, N. Barnett, A. Baty, C. Bennett, N. Brandman-hughes, R. Cavanaugh, S.J. Das, R. Escobar Franco, O. Evdokimov, C.E. Gerber, H. Gupta, M. Hawksworth, A. Hingrajiya, D.J. Hofman, Z. Huang, J.h. Lee, C. Mills, S. Nanda, G. Nigmatkulov, B. Ozek, V. Pant, T. Phan, D. Pilipovic, R. Pradhan, E. Prifti, T. Roy, D. Shekar, N. Singh, F. Strug, A. Thielen, M.B. Tonjes, N. Varelas, M.A. Wadud, A. Wang, J. Yoo

The University of Iowa, Iowa City, Iowa, USA
M. Alhusseini, D. Blend, K. Dilsiz[85], O.K. Köseyan, A. Mestvirishvili[56], O. Neogi, H. Ogul[86], Y. Onel, A. Penzo, C. Snyder

Johns Hopkins University, Baltimore, Maryland, USA
B. Blumenfeld, J. Davis, A.V. Gritsan, Z. Huang, L. Kang, P. Maksimovic, N. Pinto, M. Roguljic, S. Sekhar, M.V. Srivastav, M. Swartz

The University of Kansas, Lawrence, Kansas, USA
A. Abreu, L.F. Alcerro Alcerro, J. Anguiano, S. Arteaga Escatel, P. Baringer, A. Bean, R. Bhattacharya, M. Chukwuka, Z. Flowers, D. Grove, J. King, G. Krintiras, M. Lazarovits, C. Le Mahieu, J. Marquez, M. Murray, M. Nickel, E. Reynolds, C. Rogan, C. Royon, S. Rudrabhatla, S. Sanders, G. Wilson

Kansas State University, Manhattan, Kansas, USA
A. Ahmad, B. Allmond, N. Islam, A. Ivanov, K. Kaadze, Y. Maravin, J. Natoli, G.G. Reddy, D. Roy, G. Sorrentino

University of Maryland, College Park, Maryland, USA
Z. Alton, A. Baden, A. Belloni, J. Bistany-riebman, S.C. Eno, N.J. Hadley, S. Jabeen, R.G. Kellogg, T. Koeth, B. Kronheim, S. Lascio, J. Lee, P. Major, A.C. Mignerey, C. Palmer, C. Papageorgakis, M.M. Paranjpe, E. Popova[87], A. Shevelev, M. Wrotny, L. Zhang

Massachusetts Institute of Technology, Cambridge, Massachusetts, USA
C. Baldenegro Barrera, H. Bossi, S. Bright-Thonney, I.A. Cali, Y.c. Chen, P.c. Chou, M. D'Alfonso, J. Eysermans, C. Freer, G. Gomez-Ceballos, M. Goncharov, G. Grosso, P. Harris, D. Hoang, G.M. Innocenti, K. Ivanov, G. Kopp, D. Kovalskyi, J. Lang, L. Lavezzo, Y.-J. Lee, P. Lugato, C. Mcginn, E. Moreno, A. Novak, M.I. Park, C. Paus, C. Reissel, C. Roland, G. Roland, S. Rothman, T.a. Sheng, G.S.F. Stephans, D. Walter, J. Wang, Z. Wang, B. Wyslouch, T. J. Yang, K. Yoon

University of Minnesota, Minneapolis, Minnesota, USA
A. Alpana, B. Crossman, W.J. Jackson, C. Kapsiak, D. Mahon, J. Mans, B. Marzocchi, R. Rusack, O. Sancar, R. Saradhy, N. Strobbe

University of Nebraska-Lincoln, Lincoln, Nebraska, USA
K. Bloom, D.R. Claes, S.V. Dixit, G. Haza, J. Hossain, C. Joo, I. Kravchenko, K.H.M. Kwok, Y. Mehra, J. Morris, A. Rohilla, J.E. Siado, A. Vagnerini, A. Wightman

State University of New York at Buffalo, Buffalo, New York, USA
H. Bandyopadhyay, H.w. Hsia, I. Iashvili, A. Kalogeropoulos, A. Kharchilava,

A. Mandal, C. McLean, M. Morris, D. Nguyen, O. Poncet, S. Rappoccio, H. Rejeb Sfar, W. Terrill, A. Williams, D. Yu

Northeastern University, Boston, Massachusetts, USA
A. Aarif, G. Alverson, E. Barberis, S. Bein, J. Bonilla, B. Bylsma, M. Campana, R. Clark, J. Dervan, Y. Haddad, Y. Han, I. Israr, A. Krishna, M. Lu, N. Manganelli, R. Mccarthy, D.M. Morse, T. Orimoto, L. Skinnari, C.S. Thoreson, E. Tsai, D. Wood

Northwestern University, Evanston, Illinois, USA
S. Dittmer, K.A. Hahn, S. King, D. Li, M. Mcginnis, Y. Miao, D.G. Monk, M.H. Schmitt, A. Taliercio, M. Velasco, J. Wang, D. Wilbern

University of Notre Dame, Notre Dame, Indiana, USA
G. Agarwal, R. Band, R. Bucci, S. Castells, A. Das, A. Datta, A. Ehnis, R. Goldouzian, M. Hildreth, T. Ivanov, C. Jessop, K. Lannon, J. Lawrence, L. Lutton, J. Mariano, N. Marinelli, P. Mastrapasqua, A. Masud, T. McCauley, C. Mcgrady, C. Moore, Y. Musienko[21], H. Nelson, M. Osherson, A. Piccinelli, R. Ruchti, A. Townsend, Y. Wan, M. Wayne, H. Yockey

The Ohio State University, Columbus, Ohio, USA
M. Carrigan, R. De Los Santos, L.S. Durkin, C. Hill, M. Joyce, L. Nestor, D.A. Wenzl, B.L. Winer, B. R. Yates

Princeton University, Princeton, New Jersey, USA
H. Bouchamaoui, G. Dezoort, P. Elmer, A. Frankenthal, M. Galli, B. Greenberg, K. Kennedy, Y. Lai, D. Lange, A. Loeliger, D. Marlow, I. Ojalvo, J. Olsen, F. Simpson, D. Stickland, C. Tully, S. Yoon

University of Puerto Rico, Mayaguez, Puerto Rico, USA
S. Malik, R. Sharma

Purdue University, West Lafayette, Indiana, USA
S. Chandra, A. Gu, L. Gutay, L. He, M. Huwiler, M. Jones, A.W. Jung, I.G. Karslioglu, D. Kondratyev, J. Li, M. Liu, M. Macedo, G. Negro, N. Neumeister, G. Paspalaki, S. Piperov, N.R. Saha, J.F. Schulte, R. Sharma, F. Wang, A.L. Wesolek, A. Wildridge, W. Xie, Y. Yao, Y. Zhong

Purdue University Northwest, Hammond, Indiana, USA
N. Parashar, A. Pathak, E. Shumka

Rice University, Houston, Texas, USA
D. Acosta, A. Agrawal, C. Arbour, T. Carnahan, K.M. Ecklund, F.J.M. Geurts, I. Krommydas, N. Lewis, W. Li, J. Lin, X. Liu, C. Loizides, O. Miguel Colin, B.P. Padley, R. Redjimi, J. Rotter, C. Vico Villalba, M. Wulansatiti, E. Yigitbasi, Y. Zhang

University of Rochester, Rochester, New York, USA
O. Bessidskaia Bylund, A. Bodek, P. de Barbaro†, R. Demina, A. Garcia-Bellido, H.S. Hare, O. Hindrichs, N. Parmar, P. Parygin[87], H. Seo, R. Taus, Y.h. Yu

Rutgers, The State University of New Jersey, Piscataway, New Jersey, USA
B. Chiarito, J.P. Chou, S.V. Clark, S. Donnelly, D. Gadkari, Y. Gershtein, E. Halkiadakis, C. Houghton, D. Jaroslawski, A. Kobert, I. Laflotte, A. Lath, J. Martins, P. Meltzer, M. Perez Prada, K. Ramdin, B. Rand, J. Reichert, P. Saha,

S. Salur, S. Somalwar, R. Stone, S.A. Thayil, S. Thomas, A. K. Virdi, J. Vora

University of Tennessee, Knoxville, Tennessee, USA
A. Abdelhamid, D. Ally, A.G. Delannoy, S. Fiorendi, J. Harris, T. Holmes, A.R. Kanuganti, N. Karunarathna, J. Lawless, L. Lee, E. Nibigira, B. Skipworth, S. Spanier, C. Thompson, A. Vendrasco

Texas A&M University, College Station, Texas, USA
D. Aebi, M. Ahmad, T. Akhter, K. Androsov, A. Basnet, A. Bolshov, O. Bouhali[88], A. Cagnotta, S. Cooperstein, V. D'Amante, R. Eusebi, P. Flanagan, J. Gilmore, Y. Guo, T. Kamon, R. Mueller, G. Pizzati, A. Safonov

Texas Tech University, Lubbock, Texas, USA
N. Akchurin, J. Damgov, Y. Feng, N. Gogate, W. Jin, S.W. Lee, C. Madrid, S. Magedov, A. Mankel, T. Peltola, I. Volobouev

Vanderbilt University, Nashville, Tennessee, USA
U. Acharya, E. Appelt, Y. Chen, S. Greene, A. Gurrola, W. Johns, R. Kunnawalkam Elayavalli, A. Melo, D. Rathjens, F. Romeo, S. Tuo, J. Velkovska, J. Zhang

University of Virginia, Charlottesville, Virginia, USA
B. Cardwell, H. Chung, B. Cox, J. Hakala, G. Hamilton Ilha Machado, R. Hirosky, M. Jose, A. Ledovskoy, C. Mantilla, R. Menon Raghunandanan, C. Neu, C. Ramón Álvarez, Z. Wu

Wayne State University, Detroit, Michigan, USA
P.E. Karchin

University of Wisconsin - Madison, Madison, Wisconsin, USA
A. Aravind, S. Banerjee, K. Black, T. Bose, E. Chavez, R. Cruz, S. Dasu, P. Everaerts, C. Galloni, H. He, M. Herndon, A. Herve, C.K. Koraka, S. Lomte, R. Loveless, J. Marquez, A. Mohammadi, S. Mondal, T. Nelson, G. Parida, D. Pinna, A. Savin, V. Sharma, R. Simeon, W.H. Smith, D. Teague, M. Thakore, A. Thete, A. Warden

Authors affiliated with an international laboratory covered by a cooperation agreement with CERN
S. Afanasiev, V. Alexakhin, Yu. Andreev, D. Budkouski, R. Chistov, M. Danilov, T. Dimova, I. Gorbunov, A. Kamenev, V. Karjavine, O. Kodolova[89], V. Korenkov, I. Korsakov, A. Kozyrev, A. Lanev, A. Malakhov, V. Matveev, A. Nikitenko[90,89], V. Palichik, V. Perelygin, O. Radchenko, M. Savina, V. Shalaev, S. Shmatov, S. Shulha, Y. Skovpen, K. Slizhevskiy, V. Smirnov, O. Teryaev, A. Toropin, N. Voytishin, A. Zarubin, I. Zhizhin

Authors affiliated with an institute formerly covered by a cooperation agreement with CERN
L. Dudko, V. Kim[21], V. Murzin, V. Oreshkin, D. Sosnov

†: Deceased
[1]Also at Yerevan State University, Yerevan, Armenia
[2]Also at TU Wien, Vienna, Austria
[3]Also at Ghent University, Ghent, Belgium
[4]Also at FACAMP - Faculdades de Campinas, Sao Paulo, Brazil
[5]Also at Universidade Estadual de Campinas, Campinas, Brazil

[6]Also at Federal University of Rio Grande do Sul, Porto Alegre, Brazil
[7]Also at The University of the State of Amazonas, Manaus, Brazil
[8]Also at University of Chinese Academy of Sciences, Beijing, China
[9]Also at University of Chinese Academy of Sciences, Beijing, China
[10]Also at School of Physics, Zhengzhou University, Zhengzhou, China
[11]Now at Henan Normal University, Xinxiang, China
[12]Also at University of Shanghai for Science and Technology, Shanghai, China
[13]Also at The University of Iowa, Iowa City, Iowa, USA
[14]Also at Nanjing Normal University, Nanjing, China
[15]Also at Center for High Energy Physics, Peking University, Beijing, China
[16]Also at Helwan University, Cairo, Egypt
[17]Now at Zewail City of Science and Technology, Zewail, Egypt
[18]Also at Cairo University, Cairo, Egypt
[19]Also at Université de Haute Alsace, Mulhouse, France
[20]Also at Purdue University, West Lafayette, Indiana, USA
[21]Also at an institute formerly covered by a cooperation agreement with CERN
[22]Also at University of Hamburg, Hamburg, Germany
[23]Also at RWTH Aachen University, III. Physikalisches Institut A, Aachen, Germany
[24]Also at Bergische University Wuppertal (BUW), Wuppertal, Germany
[25]Also at Brandenburg University of Technology, Cottbus, Germany
[26]Also at Forschungszentrum Jülich, Juelich, Germany
[27]Also at CERN, European Organization for Nuclear Research, Geneva, Switzerland
[28]Also at HUN-REN ATOMKI - Institute of Nuclear Research, Debrecen, Hungary
[29]Now at Universitatea Babes-Bolyai - Facultatea de Fizica, Cluj-Napoca, Romania
[30]Also at MTA-ELTE Lendület CMS Particle and Nuclear Physics Group, Eötvös Loránd University, Budapest, Hungary
[31]Also at HUN-REN Wigner Research Centre for Physics, Budapest, Hungary
[32]Also at Physics Department, Faculty of Science, Assiut University, Assiut, Egypt
[33]Also at The University of Kansas, Lawrence, Kansas, USA
[34]Also at Punjab Agricultural University, Ludhiana, India
[35]Also at University of Hyderabad, Hyderabad, India
[36]Also at Indian Institute of Science (IISc), Bangalore, India
[37]Also at University of Visva-Bharati, Santiniketan, India
[38]Also at Institute of Physics, Bhubaneswar, India
[39]Also at Deutsches Elektronen-Synchrotron, Hamburg, Germany
[40]Also at Isfahan University of Technology, Isfahan, Iran
[41]Also at Sharif University of Technology, Tehran, Iran
[42]Also at Department of Physics, University of Science and Technology of Mazandaran, Behshahr, Iran
[43]Also at Department of Physics, Faculty of Science, Arak University, ARAK, Iran
[44]Also at Kocaeli University, KOCAELI, Turkey
[45]Also at Centro Siciliano di Fisica Nucleare e di Struttura Della Materia, Catania, Italy
[46]Also at James Madison University, Harrisonburg, Maryland, USA
[47]Also at Università degli Studi Guglielmo Marconi, Roma, Italy
[48]Also at Scuola Superiore Meridionale, Università di Napoli 'Federico II', Napoli, Italy
[49]Also at Fermi National Accelerator Laboratory, Batavia, Illinois, USA
[50]Also at Lulea University of Technology, Lulea, Sweden
[51]Also at Ain Shams University, Cairo, Egypt
[52]Also at Consiglio Nazionale delle Ricerche - Istituto Officina dei Materiali, Perugia, Italy

[53]Also at UPES - University of Petroleum and Energy Studies, Dehradun, India
[54]Also at Institut de Physique des 2 Infinis de Lyon (IP2I), Villeurbanne, France
[55]Also at Department of Applied Physics, Faculty of Science and Technology, Universiti Kebangsaan Malaysia, Bangi, Malaysia
[56]Also at Georgian Technical University, Tbilisi, Georgia
[57]Now at Boston University, Boston, Massachusetts, USA
[58]Also at Departamento de Física Instituto Superior Técnico, LISBON, Portugal
[59]Also at Trincomalee Campus, Eastern University, Sri Lanka, Nilaveli, Sri Lanka
[60]Also at Saegis Campus, Nugegoda, Sri Lanka
[61]Also at National and Kapodistrian University of Athens, Athens, Greece
[62]Also at Ecole Polytechnique Fédérale Lausanne, Lausanne, Switzerland
[63]Also at Universität Zürich, Zurich, Switzerland
[64]Also at Stefan Meyer Institute for Subatomic Physics, Vienna, Austria
[65]Also at Near East University, Research Center of Experimental Health Science, Mersin, Turkey
[66]Also at Konya Technical University, Konya, Turkey
[67]Also at Izmir Bakircay University, Izmir, Turkey
[68]Also at Adiyaman University, Adiyaman, Turkey
[69]Also at Istanbul Sabahattin Zaim University, Istanbul, Turkey
[70]Also at Marmara University, Istanbul, Turkey
[71]Also at Milli Savunma University, Istanbul, Turkey
[72]Also at Informatics and Information Security Research Center, Gebze/Kocaeli, Turkey
[73]Also at Kafkas University, Kars, Turkey
[74]Now at Istanbul Okan University, Istanbul, Turkey
[75]Also at Istanbul University - Cerrahpasa, Faculty of Engineering, Istanbul, Turkey
[76]Also at Istinye University, Istanbul, Turkey
[77]Also at Mimar Sinan University, Istanbul, Istanbul, Turkey
[78]Also at School of Physics and Astronomy, University of Southampton, Southampton, United Kingdom
[79]Also at Monash University, Faculty of Science, Clayton, Australia
[80]Also at Università di Torino, Torino, Italy
[81]Also at Karamanoğlu Mehmetbey University, Karaman, Turkey
[82]Also at California Lutheran University, Thousand Oaks, California, USA
[83]Also at California Institute of Technology, Pasadena, California, USA
[84]Also at United States Naval Academy, Annapolis, Maryland, USA
[85]Also at Bingol University, Bingol, Turkey
[86]Also at Sinop University, Sinop, Turkey
[87]Now at another institute formerly covered by a cooperation agreement with CERN
[88]Also at Hamad Bin Khalifa University (HBKU), Doha, Qatar
[89]Also at Yerevan Physics Institute, Yerevan, Armenia
[90]Also at Imperial College, London, United Kingdom